

Sensitivity of Holocene atmospheric CO₂ and the modern carbon budget to early human land use: analyses with a process-based model

B. D. Stocker^{1,2}, K. Strassmann^{1,2,*}, and F. Joos^{1,2}

¹Climate and Environmental Physics, Physics Institute, University of Bern, Switzerland

²Oeschger Centre for Climate Change Research, University of Bern, Switzerland

* now at: National Institute for Environmental Sciences, Center for Global Environmental Research, Tsukuba-City, Japan

Received: 28 January 2010 – Published in Biogeosciences Discuss.: 5 February 2010

Revised: 9 December 2010 – Accepted: 31 December 2010 – Published: 17 January 2011

Abstract. A Dynamic Global Vegetation model coupled to a simplified Earth system model is used to simulate the impact of anthropogenic land cover changes (ALCC) on Holocene atmospheric CO₂ and the contemporary carbon cycle. The model results suggest that early agricultural activities cannot explain the mid to late Holocene CO₂ rise of 20 ppm measured on ice cores and that proposed upward revisions of Holocene ALCC imply a smaller contemporary terrestrial carbon sink. A set of illustrative scenarios is applied to test the robustness of these conclusions and to address the large discrepancies between published ALCC reconstructions. Simulated changes in atmospheric CO₂ due to ALCC are less than 1 ppm before 1000 AD and 30 ppm at 2004 AD when the HYDE 3.1 ALCC reconstruction is prescribed for the past 12 000 years. Cumulative emissions of 69 GtC at 1850 and 233 GtC at 2004 AD are comparable to earlier estimates. CO₂ changes due to ALCC exceed the simulated natural interannual variability only after 1000 AD. To consider evidence that land area used per person was higher before than during early industrialisation, agricultural areas from HYDE 3.1 were increased by a factor of two prior to 1700 AD (scenario H2). For the H2 scenario, the contemporary terrestrial carbon sink required to close the atmospheric CO₂ budget is reduced by 0.5 GtC yr⁻¹. Simulated CO₂ remains small even in scenarios where average land use per person is increased beyond the range of published estimates. Even extreme assumptions for preindustrial land conversion and high per-capita land use do not result in simulated CO₂ emissions that are sufficient to explain the magnitude and the timing of the late Holocene CO₂ increase.

1 Introduction

Atmospheric CO₂ varies within 172–300 ppm over glacial-interglacial cycles (Lüthi et al., 2008), with higher concentrations during interglacial periods. The current interglacial, the Holocene, is characterized by an increase in atmospheric CO₂ during the last 8000 years (8 kyr) (see Fig. 2, bottom) and an accelerating increase in atmospheric CH₄ since 3 kyr before present (BP). This has stimulated a debate about the underlying causes and mechanisms (e.g., Indermühle et al., 1999; Broecker et al., 2001; Brovkin et al., 2002; Ruddiman, 2003; Joos et al., 2004; Elsig et al., 2009). Anthropogenic land cover change (ALCC) has been proposed as a contributing factor. The clearing of natural vegetation for agriculture begins with the first neolithic settlements some ten thousand years before present (Williams, 2003). Over the course of millennia, humans have adopted a sedentary and agricultural lifestyle in different parts of the earth. This triggered an increase in population densities and further drove the demand for cultivatable land (Diamond, 2002). Even long before industrialisation, ALCC could have affected climate and atmospheric chemistry through (i) carbon emissions and the associated changes in radiative forcing, (ii) changes in the local to regional albedo and the hydrological balance, and (iii) changes in the emissions of non-CO₂ greenhouse agents, carbon monoxide, and volatile organic carbon compounds (Betts et al., 2007; Bonan, 2008).

Ruddiman (2003, 2007) attributed the reconstructed 20 ppm increase in atmospheric CO₂ after 8 kyr BP to agricultural activities and an assumed climate-carbon cycle feedback. This “early anthropogenic” hypothesis is not supported by published estimates of anthropogenic carbon emissions prior to the industrial period and their simulated airborne



Correspondence to: B. D. Stocker
(beni@climate.unibe.ch)

fractions (Joos et al., 2004; Strassmann et al., 2008), which are all too low to explain the observed trend and imply a smaller anthropogenic impact. In simulations by Pongratz et al. (2009b), ALCC did not cause an increase of atmospheric CO₂ above natural variability before late medieval times, with an average preindustrial airborne fraction of ALCC emissions of 21% (800–1850 AD).

Inverse modelling based on recently published high resolution $\delta^{13}\text{C}$ measurements on the Antarctic Dome C ice core constrains the net contribution of Holocene changes in terrestrial carbon storage to the observed CO₂ rise to 36 ± 37 GtC or 3 ppm since 5 kyr BP (Elsig et al., 2009). However, a hypothetical, extensive early ALCC-related carbon source and its associated CO₂ and $\delta^{13}\text{C}$ signals could be masked by the net effect of other terrestrial carbon sources and sinks. For example, recent studies show large increases in peat carbon storage over the Holocene (MacDonald et al., 2006; Yu et al., 2010). These studies rely on data from currently existing peat reservoirs and do not consider carbon releases from peatlands that may have been lost. Different estimates of carbon storage in boreal peat deposits vary by a factor of two (Yu et al., 2010; Tarnocai et al., 2009). Peat formation represents one of several processes affecting terrestrial carbon inventories. This leaves a range of possible ALCC histories and requires the implementation of explicit ALCC scenarios in terrestrial carbon cycle models to further constrain the human impact on atmospheric CO₂.

Published reconstructions for preindustrial ALCC (Klein Goldewijk, 2001; Klein Goldewijk and van Dreht, 2006; Olofsson and Hickler, 2008; Pongratz et al., 2008; Kaplan et al., 2009, 2011) exhibit large discrepancies (see also Gaillard et al., 2010). As a result, the human impact on terrestrial carbon stocks, atmospheric CO₂, and climate in the Holocene is highly uncertain. Direct historical or archaeological information is scarce, and spatial extrapolation of proxy records from natural archives to a global scale remains challenging (Gaillard et al., 2010). Thus, the HYDE 3.1 reconstruction of ALCC (Klein Goldewijk, 2001; Klein Goldewijk and van Dreht, 2006), as well as the similar “best-guess” reconstruction that was used in the study of Pongratz et al. (2009b), rely on population maps as a proxy for agricultural areas and the assumption that the agricultural land area required to support a given population is constant (land area per person, LAP). Pongratz et al. (2008) presented alternative ALCC scenarios that take into account the effects of technological advances and associated increases in land productivity. Unfortunately, no scenario with high early land use areas and accordingly slower land cover dynamics in the centuries before Industrialisation has been used to simulate the effect on atmospheric CO₂.

The assumption of a constant LAP is questionable. If a generally decreasing trend in LAP throughout the Holocene is correct, constant LAP assumptions may lead to an underestimation of the area affected by preindustrial ALCC and of early ALCC-related CO₂ emissions and atmospheric CO₂

changes. Ruddiman and Ellis (2009) argued that this reopens the case of their early anthropogenic hypothesis.

Indeed, various lines of evidence point towards a low bias of the above mentioned ALCC estimates. Kaplan et al. (2009) analyzed historical data on population density and forest cover for several European countries. They derived an expression in which LAP is a function of population *density* and thus changes with time. According to their reconstruction of European ALCC back to 1000 BC, the European landscape was already dominated by humans two thousand years ago, and was largely deforested by 1000 AD, when open land made up more than 70% across much of Western Europe. Pollen analyses and historical work (e.g., Soepboer et al., 2010; Williams, 2003) are in line with this result. Recently, Kaplan et al. (2011) estimate that globally 10% of the available land was under anthropogenic land use by 1 AD; this is about three times more than indicated by the Hyde 3.1 data. Applying the same methodology (Kaplan et al., 2009), Gaillard et al. (2010) suggests that in 1 AD, more than 60% of available land was used for agriculture in the Yellow River, Indus, Brahmaputra, Euphrates and Tigris river valleys, as well as in Southern India, parts of Central America and along the Andes. Heavy deforestation in Medieval China has also been reported by historical studies (e.g., Murphey, 1983). A limited set of low resolution charcoal accumulation records from soils and lacustrine sediments was interpreted as an indication of considerable deforestation after 2000 BP also in the Americas (Nevle and Bird, 2008). However, the comprehensive study by Marlon et al. (2009) suggests that fire frequency and charcoal production during the last millennium co-varies with climate rather than population.

The HYDE and Pongratz et al. (2008) reconstructions are not consistent with the notions of extensive preindustrial deforestation in Europe and other parts of the world. Their assumptions of a constant LAP yields a relatively small extent of permanently cultivated areas in all of the above mentioned regions before 1000 AD.

The amount of cultivated land at any time is the net result of land use transitions (clearing and abandonment), which are not specified in, e.g., HYDE 3.1. Hurtt et al. (2006) developed spatio-temporal datasets of land use transitions from the ALCC maps by Klein Goldewijk (2001) (HYDE version 2) and Ramankutty and Foley (1999), using data on wood harvest and assumptions on land use preferences across the world. The Hurtt et al. (2006) datasets capture land use patterns such as shifting cultivation and wood harvest, albeit with large uncertainty. In simulations with a dynamic land model, shifting cultivation practices in the tropics increased land carbon loss by up to 50% over the last 300 years (yr) (Shevliakova et al., 2009) as compared to a simulation with permanent agriculture only. In the study of Olofsson and Hickler (2008) cumulative emissions between 4000 BC and 1990 AD are enhanced by 35% when non-permanent agriculture is considered. At earlier times, non-permanent agriculture was more widespread than today. At the same time,

low population densities and accordingly long rotation periods (the time until the same plot is cultivated again) caused smaller losses of soil carbon (Brady, 1996) and enabled a more complete recovery of woody vegetation as compared to present-day shifting cultivation systems. For the period before 1850, Kaplan et al. (2011) find differences in carbon emissions of around 15% between simulations with and without a representation of shifting cultivation. Due to the paucity of data, in particular for the preindustrial era, shifting cultivation, wood harvest, forest management, and their impacts on the terrestrial carbon cycle are not captured in many studies (Strassmann et al., 2008; Pongratz et al., 2008), including the present one.

The low bias which stems from neglecting variations in LAP and the effects of shifting cultivations, as well as the discrepancies between different ALCC estimates results in a high uncertainty of estimates for historical ALCC emissions and has precluded a precise quantification of the preindustrial human impact on the carbon cycle. Earlier studies on ALCC have not fully addressed this uncertainty. In addition, they are restricted to the past millennium (Brovkin et al., 2006; Pongratz et al., 2009b), assess only the total cumulative carbon emissions before industrialization (Joos et al., 2004; Strassmann et al., 2008), do not model carbon accumulation in the atmosphere (Olofsson and Hickler, 2008; Kaplan et al., 2011) or are of highly qualitative nature (Ruddiman, 2003, 2007; Williams, 2003; Nevle and Bird, 2008).

Here, we present transient simulations of the impact of preindustrial land use change on atmospheric CO₂ throughout the Holocene based on spatially explicit ALCC maps. An assessment of uncertainty in the evolution of ALCC and its implications for the modern carbon budget is included.

The Bern Carbon Cycle-Climate Model (BernCC) is forced by explicitly prescribing the evolution of croplands, pastures, and urban areas over the past 12 kyr. As a standard scenario we use the HYDE 3.1 reconstruction. The extent of a possible low bias in the HYDE data and in the simulated impact on the carbon cycle is constrained using three complementary ALCC scenarios. Sensitivity of the atmospheric CO₂ increase to different rates of land conversion is analyzed using a schematic scenario with linearly increasing land use areas. Due to a lack of more detailed data for early Holocene ALCC and land use practices, we use highly stylized scenarios and address the effects of shifting cultivation and forest management practices on CO₂ emissions implicitly. The simulated impact of soil cultivation and crop harvesting on carbon emissions and atmospheric CO₂ is quantified. Finally, we examine this scenario range for its consistency with available information on LAP and with the carbon budget of the last millennium as inferred from a single deconvolution analysis (Siegenthaler and Oeschger, 1987).

2 Methods

2.1 ALCC scenarios

The standard scenario for historical ALCC is defined by the spatially aggregated HYDE 3.1 data (HY) (Klein Goldewijk, 2001; Klein Goldewijk and van Drecht, 2006; HYDE 3.1, 2008). In addition, three alternative ALCC histories (Fig. 1) are used to illustrate and explore the sensitivity of carbon emissions and atmospheric CO₂ to different evolutions of ALCC. The scenarios are identical with respect to the land use area at 10 000 BC and 2005 AD. This is motivated by the premise that permanent agriculture was practically not existent at 10 000 BC and by the relatively high quality and reliability of present-day data.

The spatial aggregation of the HYDE data for the application in the BernCC modelling framework ($3.75^\circ \times 2.5^\circ$ spatial resolution) is described in (Strassmann et al., 2008). The HYDE ALCC data define the relative share of croplands, pastures and urban areas in each grid cell at 58 time steps between 10 000 BC and 2005 AD. The temporal resolution is millennial before 1 AD, centennial until 1700 AD, and decadal thereafter. HYDE uses a LAP pattern which is roughly constant throughout the entire preindustrial Holocene. Thus, regional land use area is directly proportional to regional population as long as unused land is available. Uncertainties in population numbers are propagated to estimated land use areas. An average value for LAP can be derived by dividing the global land use area by the global population number (Klein Goldewijk, 2001; Klein Goldewijk and van Drecht, 2006); this yields 1.0–1.3 ha/pers. (hectares per person) (see also Table 2).

In scenario H2, agricultural areas from HYDE are scaled by a factor of 2 before 1700 AD. After 1700, the scaling factor linearly decreases to 1 until 2005 AD. H2 represents generally larger preindustrial land use areas than the maximum scenario presented by Pongratz et al. (2008). In H2, up to 70% of the land area is under anthropogenic use in Europe by 1000 AD compared to about 40% in the HY scenario. European land use areas in H2 are roughly in line with the reconstruction of Kaplan et al. (2009).

The overshoot scenario (OS) represents the same spatial distribution of land use areas as in HY, but area fractions before 1700 AD are scaled with a time-varying factor that relates population density and the area fraction of agricultural areas in a grid cell, as defined by Eq. (1) in Kaplan et al. (2009) (see Stocker, 2009). The scaling factor is 1 for all years after 1700 AD. This relation is suggested to represent the effect of technological change on land productivity and hence on the mean LAP. As a result, global total land use areas decline sharply after Medieval times because the relative population growth is smaller than the relative decline in LAP.

Scenario LIN is purely schematic and serves as an illustration. Agricultural areas are interpolated between 10 000 BC (zero ALCC) and the state defined by the HYDE 2005 AD

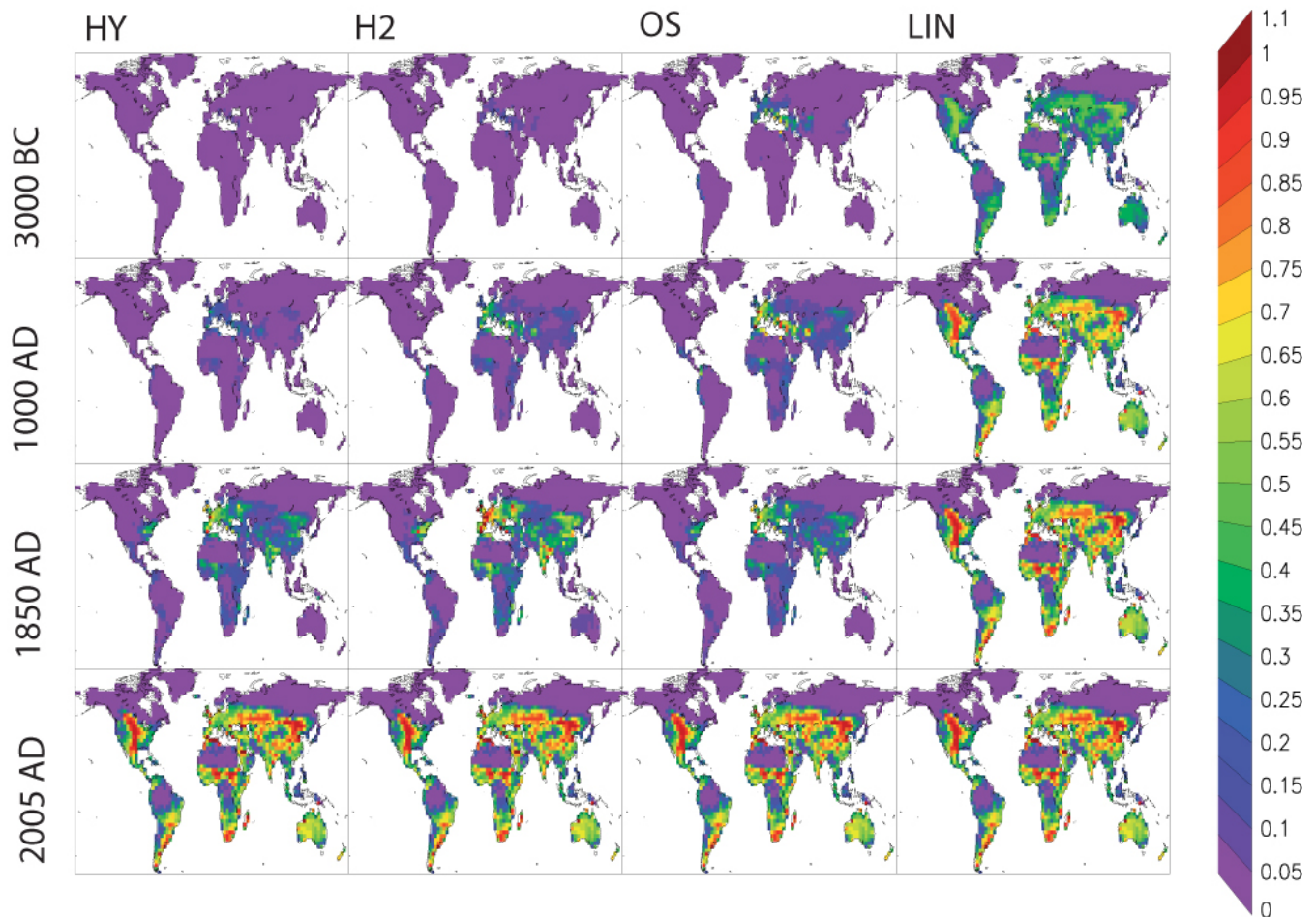


Fig. 1. Area fraction of agricultural land (sum of cropland, pastures and urban) for different scenarios and time periods on the aggregated $2.5 \times 3.75^\circ$ grid used by LPJ.

map. Thus, the spatial distribution corresponds to HYDE in 2005 at all times and accordingly, anthropogenic ALCC occurs worldwide over the entire Holocene.

To limit the share of total ALCC to 100%, the land use area according to the above scenario definitions had to be reduced for some cells. In doing so, the relative share of pastures, croplands, and urban areas, as given in HYDE, was conserved. This affected the global total land use area only slightly (Fig. 2).

In brief, our illustrative, stylized ALCC scenarios span a wide range from a scenario potentially underestimating preindustrial ALCC (HY) to a scenario with an extremely high magnitude and global extent of anthropogenic ALCC in the Holocene (LIN). The resilience of carbon pools after land abandonment is addressed by the overshoot scenario (OS).

2.2 Model description and setup

The ALCC simulations are performed with the BernCC model (Joos et al., 2001; Gerber et al., 2003; Strassmann

et al., 2008). BernCC is a simplified Earth system model, which includes the Lund-Potsdam-Jena Dynamical Global Vegetation Model (LPJ-DGVM, Sitch et al., 2003) with an ALCC component by Strassmann et al. (2008). LPJ simulates terrestrial carbon assimilation and respiration in response to variations in CO₂ and climate. It exchanges net carbon fluxes with a well-mixed atmosphere and a Mixed-Layer Pulse-Response representation of the HILDA ocean model (Joos et al., 1996), which also parametrizes carbonate-sediment interactions (Joos et al., 2004). The coupled modelling framework simulates the evolution of atmospheric CO₂ at low computational costs.

In an earlier study that considered climatic variations on the millennial time scale but no explicit representation of ALCC, the simulated increase in terrestrial carbon storage is in the range of 820 to 850 GtC over the past 20 kyr, and 28 to 75 GtC over the past 6 kyr (Joos et al., 2004). These effects are largely independent of ALCC-related effects, as ascertained with simulations driven by variable ALCC and natural changes. Here, for simplicity of interpretation, we

keep all boundary conditions other than ALCC constant. In other words, climate is constant throughout the simulation.

We use the Climate Research Unit's (CRU) TS 2.1 climatology from 1900 to 1930 (New et al., 1999; Mitchell and Jones, 2005), present-day land-ice distribution (Peltier, 1994; Joos et al., 2004), and the insolation at 1950 AD (Berger, 1978). The CRU climatology is repeated every 31 yr to simulate interannual variability in terrestrial carbon storage. Atmospheric CO₂ is initialized at 263 ppm and evolves in response to the terrestrial and oceanic carbon balance.

ALCC-related carbon emissions and related changes in atmospheric CO₂ are explicitly modeled by our version of LPJ using a fractional grid cell approach to distinguish different land classes (see Strassmann et al., 2008). Only the net change (difference of deforestation and abandonment) within one grid cell is simulated. Croplands and pastures are claimed from forests and natural grasslands according to their respective area shares on natural land, as simulated by LPJ.

After land conversion, tree plant functional types are suppressed from growing and urban areas are assumed to be void of any biomass. Carbon from woody biomass is partly released to the atmosphere (25%), the rest is split evenly to two product pools that decay with turnover times of 2 and 20 yr. The assessment of ALCC emissions on decadal to millennial time scales is not sensitive to the respective values. Carbon from leaves, sapwood and roots enters the litter pools of the appropriate anthropogenic land use area.

The ALCC component of Strassmann et al. (2008) does not include formulations to account for crop harvest and increased oxidation of soil organic matter associated with tillage. Here, a management parametrization is implemented following the approach of Olofsson and Hickler (2008). These authors reduce the fraction of the litter decomposition flux that is transferred to the soils from 30% to 20%. Here, we further reduce this fraction to 17% and thus increase the reduction of soils carbon pools and increase land use emissions to better reproduce the observed impact of cultivation on cropland soils (Davidson and Ackerman, 1993; Guo and Gifford, 2002; Murty et al., 2002; Ogle et al., 2005).

In addition to this standard treatment, we run sensitivity simulations where an alternative implementation of harvest is used or where agricultural management is neglected. The alternative harvest scheme follows the approach of Shevliakova et al. (2009). 100% of the leaf mass is harvested annually on croplands and 25% on pastures. 90% of the biomass harvested is oxidized directly, the rest enters the litter pools.

The model is spun up to equilibrium; model drifts in atmospheric CO₂ and carbon inventories are negligible. Simulations are carried out in (i) the standard setup and (ii) with suppressed CO₂ fertilization. We distinguish net and primary ALCC emissions. Primary ALCC emissions are defined as the net carbon fluxes to the atmosphere in a ALCC simulation with suppressed fertilization, minus a corresponding simulation without ALCC. Net emissions differ from primary emis-

sions primarily due to the CO₂ fertilization feedback as defined by Strassmann et al. (2008). Additional feedbacks due to climate variations are implicitly neglected by the setup; the "lost sinks/sources" flux (Strassmann et al., 2008) is small due to the neglect of fossil emissions and the corresponding relatively small variations in CO₂.

The set of plant functional types (PFT) and PFT-specific parameters have been updated from the version by Sitch et al. (2003) as used by Strassmann et al. (2008) and Joos et al. (2004). The new parameters proposed by Wania (2007) are used here in order to achieve a better representation of the vegetation distribution in northern latitudes. As a consequence, ALCC emissions are reduced as compared to the version of Strassmann et al. (2008) (see Sect. 4.1 for a discussion).

In addition to the parameter changes, we use a different baseline climatology (CRU TS 2.1 instead of Leemans and Cramer, 1991). Together, these updates reduce the simulated ALCC-related carbon emissions over the last 300 yr by about 30% when neglecting harvest as compared to a corresponding simulation based on the original parameters of Sitch et al. (2003) (see Strassmann et al., 2008).

2.3 Closing the global carbon budget and the quantification of a residual terrestrial sink

ALCC emissions have implications for the atmospheric CO₂ budget, for the stable isotope ¹³C, and for the magnitude of carbon sink processes. In turn, the consistency of different ALCC emissions scenarios with the atmospheric CO₂ and ¹³CO₂ evolutions offers an additional means to check the plausibility of ALCC scenarios. Here, we focus on the CO₂ budget of the last millennium and the 20th century as the earlier millennial-scale Holocene CO₂ variations are influenced by a number of not exactly quantified natural carbon fluxes (e.g., Elsig et al., 2009; Kleinen et al., 2010).

Previous analyses (Joos and Bruno, 1998; Joos et al., 1999; Trudinger et al., 2002; Houghton et al., 2004) of the ice core CO₂ and ¹³CO₂ records (Francey et al., 1999) suggest that multi-decadal net ocean-atmosphere and land biosphere-atmosphere fluxes were relatively small (<0.2 GtC yr⁻¹) during the preindustrial millennium and that the net flux from the land biosphere to the atmosphere is comparable to ALCC emissions estimated by Houghton (2003) for the 19th century. In contrast, a residual sink flux on the order of -1 to -2 GtC yr⁻¹ (negative numbers denote an uptake by the land biosphere) is required to close the CO₂ budget over the more recent decades (Denman et al., 2007); this residual sink flux is linked to the land biosphere and to processes such as unaccounted vegetation regrowth in northern mid-latitudes and possibly stimulated by increased terrestrial photosynthesis due to elevated atmospheric CO₂, as well as nitrogen input into terrestrial systems (Prentice et al., 2001; Denman et al., 2007). The intention is then not only to check the plausibility of the ALCC scenarios, but also to address the implications

of different preindustrial ALCC scenarios for the 20th century residual carbon sink flux.

Technically, we follow the single deconvolution approach of Siegenthaler and Oeschger (1987) and consider the CO₂ budget only. This is permissible for the period of the last 1000 yr as analyses of the combined CO₂ and ¹³CO₂ yield very similar results (Joos et al., 1999). The net land biosphere-to-atmosphere flux, $F_{\text{ba,net}}$, is taken from Joos et al. (1999). It is quantified by taking the difference from reconstructed changes in atmospheric CO₂ (Etheridge et al., 1996; Keeling et al., 1993; Keeling and Whorf, 2003), dN_{a}/dt , carbon emission from fossil fuels and cement production (Marland et al., 2006), E_{foss} , and the net sea-to-atmosphere flux, $F_{\text{sa,net}}$ as computed under prescribed CO₂ with the BernCC model. Net fluxes to the atmosphere are generally defined positive.

$$F_{\text{ba,net}} = \frac{d}{dt} N_{\text{a}} - E_{\text{foss}} - F_{\text{sa,net}} \quad (1)$$

The residual terrestrial sink, F_{sink} is then, as in Denman et al. (2007), the difference between the net biosphere-to-atmosphere flux and the primary carbon emissions by ALCC, E_{ALCC} :

$$F_{\text{sink}} = F_{\text{ba,net}} - E_{\text{ALCC}} \quad (2)$$

Uncertainties (1-sdv) in the sink flux related to uncertainties in the ocean model, in fossil emission estimates, and in the ice core CO₂ data have been estimated to be about 0.2 GtC yr⁻¹ for the 1800 to 1960 period (Bruno and Joos, 1997).

3 Results

Cumulative net ALCC emissions between 10 000 BC and 2004 AD add up to 159 to 192 GtC, depending on the scenario (Fig. 2). There remains a difference despite the fact that all scenarios converge to the same area under human use by 2004 AD. Differences occur due to (i) the long equilibration time of soil carbon after land conversion and (ii) differences in simulated CO₂ and the associated fertilization feedback and (iii) the size of the product pools towards the end of the simulation period (see also Fig. 3). Cumulative primary emissions in year 2004, excluding any ALCC-related feedback flux are in the range of 233 to 247 GtC (Table 1). The evolution of ALCC emissions varies considerably between different scenarios (Fig. 2, middle). Cumulative net emissions range from 47 to 190 GtC and primary emissions from 69 to 231 GtC by 1850. This scenario spread is mainly related to differences in the area under land use.

Differences in the temporal evolution of ALCC have long-term implications for emissions. This is illustrated by comparing the HY and the OS scenario. The “overshoot” scenario OS features a larger area under land use than HY before 1700 AD. In 1700 AD, the two scenarios converge and

are identical in terms of land use area thereafter. The decline in global land use areas in OS after the Medieval period is associated with a delayed and an incomplete recovery of carbon stocks on areas previously under land use. Although land use areas are identical in OS and HY throughout the industrial period, a difference in cumulative emissions of about 13 GtC still persists at present. This is a consequence of the long equilibration time scales of soil carbon stocks to a change in the input flux. Similarly, the linear ALCC scenario LIN results in higher cumulative emissions than HY and H2. In the latter scenarios, the bulk of ALCC is allocated in the industrial period and soil carbon has not yet fully adjusted to lower levels.

The simulated increase in atmospheric CO₂ (Fig. 2, bottom) depends on the ALCC scenario. Differences are substantial even by the end of the simulations in 2004 AD, when all scenarios are identical with respect to the total land area under human use. Simulated changes in CO₂ are 29, 27, 28 and 10 ppm for HY, H2, OS, and LIN, respectively. These differences are much larger than the differences in primary emissions. They are, as explained further below, related to the time scales of ocean carbon uptake. The increase over the period 1850 to 2004 is in the range of 0 to 22 ppm. By 1700 AD, the simulated CO₂ increase relative to the start of the simulation is in the range of 1 to 10 ppm for the four scenarios. The preindustrial ALCC-related atmospheric CO₂ increase remains smaller than 12 ppm, even when suppressing CO₂ fertilization.

The ice core records (Monnin et al., 2001) show that atmospheric CO₂ increased by ~20 ppm from 5000 BC to 1 AD, followed by a period with roughly constant concentrations (Fig. 2, bottom). Before 1 AD, simulated cumulative emissions are 49 GtC in OS, the scenario with the highest ALCC at that time, and the associated atmospheric CO₂ increase is less than 3 ppm. Somewhat larger CO₂ concentrations changes are simulated when CO₂ fertilization is suppressed (Fig. 2, thin lines). Thus, simulated CO₂ changes due to ALCC explain less than 20% of the reconstructed 20 ppm CO₂ increase, even in a scenario where an average LAP of more than 9 ha/pers. is assumed. This LAP value is beyond the range of published estimates (see Table 2). E.g., Ruddiman and Ellis (2009) propose 4 ± 2 ha/pers. at 5000 BC.

Area under land use peaks around 1 AD in the overshoot scenario OS and decreases thereafter until 1400 AD. The related uptake of carbon draws down atmospheric CO₂. Simulated CO₂ changes become even smaller than in HY, although the respective cumulative emissions are higher in OS than in HY at all times. This difference in CO₂ is related to the timescales of ocean uptake and the increase in cumulative emissions in HY and the decrease in OS after 1000 AD.

Harvest and soil cultivation on croplands affects the local carbon balance and leads to enhanced ALCC-related CO₂ emissions. Reductions in soil carbon are partly offset by enhanced NPP on croplands and pastures relative to the natural vegetation and correspondingly larger carbon inputs from

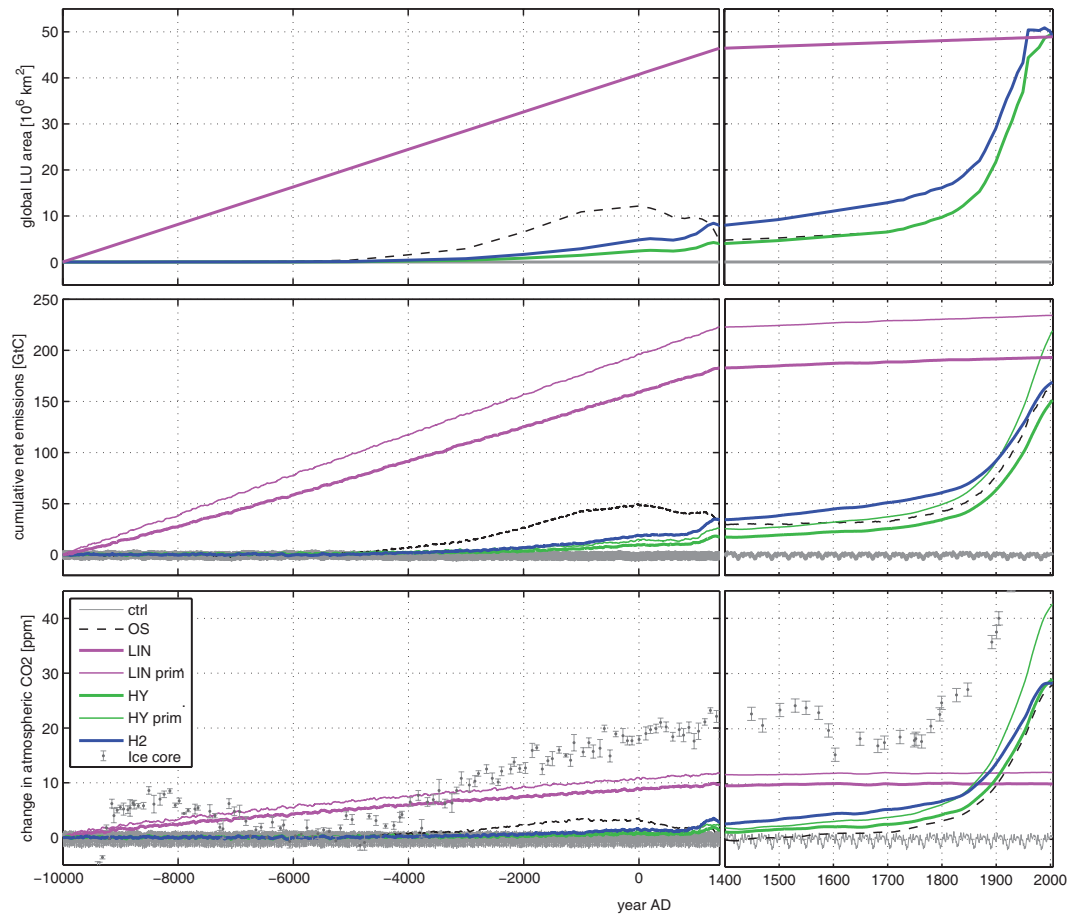


Fig. 2. Evolution of global land use area, ALCC related carbon emissions, and changes in atmospheric CO₂ over the Holocene for four ALCC scenarios (HY, H2, OS, LIN). Top: global total area of agricultural land (sum of croplands, pastures and urban). Middle: cumulative net emissions (including CO₂ fertilization feedback). Additionally, the primary emissions of HY and LIN are given by the thin lines. Bottom: Change in atmospheric CO₂ concentration relative to the concentration at the start of the simulation (263 ppm). CO₂ increase without the fertilization feedback is given by the thin lines. CO₂ anomalies relative to 8 kyr BP (259 ppm) measured on the EPICA Dome C ice core (Monnin et al., 2001) (left panel) and Law Dome (Etheridge et al., 1996) (right panel) are depicted by the grey symbols with 2- σ error bars. Time series of cumulative emissions and CO₂ anomalies represent 31-yr running averages. The simulated natural interannual variability in response to climatic variations is illustrated by the light grey curve.

biomass turnover. Soil management leads to an increase in cumulative emissions by 33% (HY) to 53% (LIN). Cumulative net emissions range between 119 to 125 GtC in 2004 without management compared to 159 to 192 GtC in the standard model setup where management is included. At 1700 AD, the atmospheric CO₂ increase due to anthropogenic land use ranges between 2 and 7 ppm when management is neglected compared to 3 to 10 ppm in the standard model setup. An implementation of harvest on agricultural land following Shevliakova et al. (2009) yields very similar results for cumulative global emissions (see Table 1), but exhibits a different spatial pattern with soil carbon gains on croplands by up to 60% in the tropics. This accumulation is compensated by smaller carbon stocks on pastures com-

pared to the standard treatment, where pasture harvest is not considered.

ALCC emissions are redistributed between the biosphere, the ocean/sediment system and the atmosphere. On millennial time scales, most of the emissions are absorbed by the ocean and ocean-sediment interactions as a consequence of the very well-understood carbonate chemistry and the dynamic mixing to depth. This is documented extensively in the literature (e.g., Joos et al., 1996; Archer et al., 1997; Cao et al., 2009). Only about 14% of an initial perturbation of the preindustrial atmosphere by a (small) carbon input remains airborne when the atmosphere-ocean system has attained a new equilibrium one to two thousand years after the emission. This airborne fraction is further lowered to 6 to 7% on

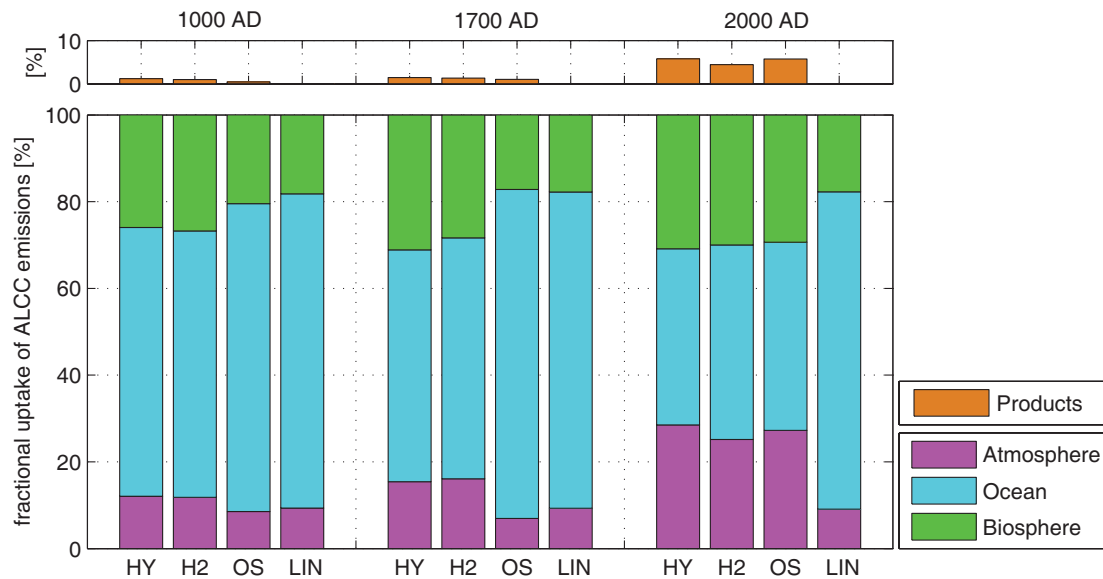


Fig. 3. Simulated redistribution of carbon emissions from anthropogenic land cover change between the atmosphere (purple), ocean (blue), the land biosphere (green), and product pools (orange, upper panel) for 1000 AD (left), 1700 AD (middle), and 2000 AD (right) and for four ALCC scenarios. Values represent fractions in percentage of cumulative emissions, including the delayed emissions from product pools. Values are averages over the 31-year period prior to the labelled year. The uptake by the land biosphere is due to CO₂ fertilisation.

a multi-millennial time scale by ocean-sediment interactions. Consequently, the airborne fraction is low in our simulations (9% to 16%) at preindustrial times for all four scenarios as the time scales over which carbon emissions occur are multi-millennial (Fig. 3).

The airborne fraction depends inter alia on the growth rate of emissions. The higher the growth rate, the higher the airborne fraction. For a high growth rate scenario the share of more recent emissions on total emissions is higher at any given point in time compared to low growth rate scenarios. Less time is effectively available for the ocean and the land to take up excess CO₂ under high growth in emissions. Thus, the airborne fraction is higher in the exponential-like increasing HY and H2 ALCC scenarios than in the linear LIN scenario. At 2000 AD, the simulated airborne fraction is 29, 25, 27 and 9% in HY, H2, OS and LIN, respectively. Similarly, the airborne fraction in OS is lower at 1000 AD, as well as 1700 AD than for HY. The relatively high airborne fraction for HY reflects that the bulk of the ALCC occurs in the last two centuries in this scenario. On the other hand, scenarios with large early ALCC are associated with a lower airborne fraction.

Next, the atmospheric CO₂ budget and the residual sink is quantified for the last millennium (Fig. 4). The residual sink is close to zero between 1005 and 1700 AD in all scenarios. Remaining deviations of up to $\pm 0.3 \text{ GtC yr}^{-1}$ may be linked to uncertainties in input data and the impact of unaccounted climatic variations on the carbon cycle. The pre-1850 AD ALCC emissions simulated for all four scenarios are compatible with the reconstructed evolution of CO₂ dur-

ing this period. The residual sink flux for HY, H2 and OS remains small until the late 19th century. In other words, the ALCC emissions of these three scenarios are compatible with the evolution of atmospheric CO₂ and current process understanding. No additional, unknown carbon flux needs to be invoked to close the carbon budget prior to the late 19th century, suggesting that last millennium ALCC emissions of these three scenarios are of realistic magnitude until this time. Relatively high simulated ALCC emissions between the 1880 and 1940 AD in HY, H2 and OS require a residual sink of about 30 GtC to close the carbon budget. In contrast, low ALCC emissions in LIN throughout the industrial period yield a residual terrestrial source of carbon of about 70 GtC between 1700 and 1930 AD.

The magnitude of early ALCC has implications for the current carbon budget. This is illustrated by the difference between the HY and H2 scenarios. H2 implies a smaller terrestrial sink than HY due to slower land conversion rates and associated lower primary emissions during the second part of the 20th century. The average residual sink flux for the 1980s is -1.7 and -1.3 GtC yr^{-1} for the HY and H2 scenarios, respectively. For the early 1990s, the implied sink flux increases to -2.1 and -1.6 GtC yr^{-1} in HY and H2, respectively. This indicates that the magnitude of the modern residual sink is potentially becoming smaller when revising the magnitude of preindustrial ALCC upward. This conclusion is robust with regard to uncertainties in the interactions between ALCC, climate CO₂ and nitrogen fertilization. However, ALCC rates during the past decades are well constrained by independent estimates and results based

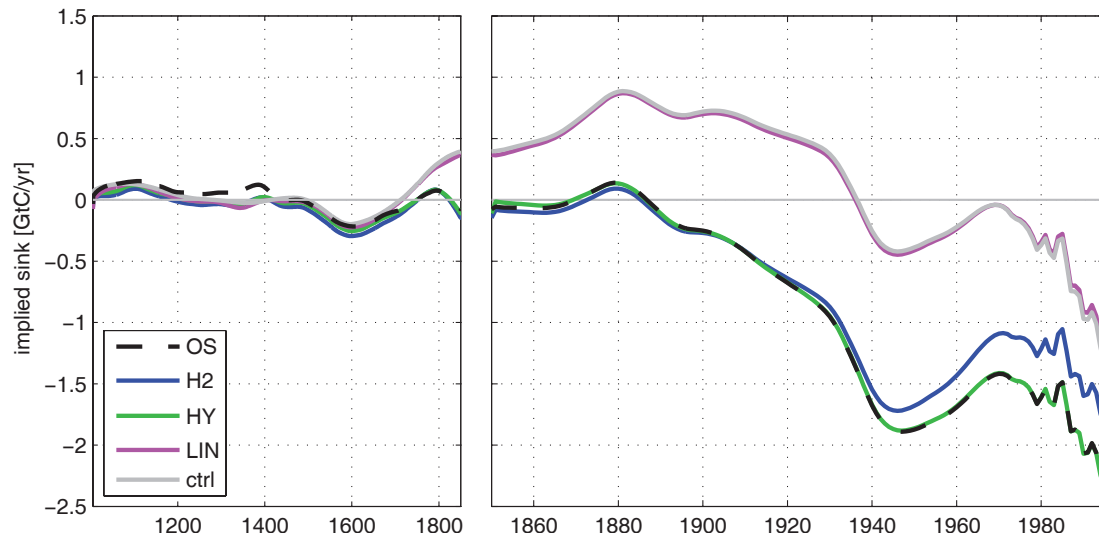


Fig. 4. Residual terrestrial carbon flux over the last millennium for four ALCC scenarios. Positive values represent a net source. The residual flux is the difference between the net atmosphere-to-land carbon flux and primary ALCC emissions. The net atmosphere-to-land flux is derived by a single-deconvolution analysis as described in Joos et al. (1999). Data are splined with a cut-off period of 300 year prior to 1850 AD and 40 year thereafter. For comparison, the residual flux for zero ALCC emissions is shown by the grey line (“ctrl”).

on the FAO statistics suggest even higher rates than in HY (Houghton, 2010).

4 Discussion

We assess the ALCC-related carbon cycle perturbation with transient simulations using the BernCC simplified Earth system model and the HYDE 3.1 data for croplands and pastures since 10 000 BC and a range of idealized scenarios. The main findings are that (i) our results do not support the hypothesis that mid to late Holocene CO₂ increase was primarily driven by ALCC and (ii) that an ALCC scenario with a larger than generally assumed share of pre- versus post-1850 AD ALCC extent and emissions considerably decreases the postulated residual sink flux in the 20th century.

Uncertainties inherent in the quantification of cumulative ALCC emissions are linked to (i) uncertainties in the distribution of terrestrial carbon inventories, (ii) uncertainties in the areas affected by anthropogenic land cover change, (iii) uncertainties in the evolution and extent of different agricultural management practices, and (iv) uncertainties in the representation of management impacts on carbon inventories. In the following sections, these uncertainties are discussed and the plausibility of different scenarios are assessed. Finally, we discuss the implications for the current carbon budget and for Holocene CO₂ and climate.

4.1 Carbon inventories and emissions

First, uncertainties related to terrestrial carbon inventories and emissions are addressed. Modeled values for above- and below-ground biomass inventory in closed forests and soil carbon content are compared to observation based estimates (Figs. 5 and 6). Simulated soil carbon is compared with the IGBP-DIS global soil carbon data set (Batjes, 2008) which represents natural as well as cultivated soils. Both, the data set as well as the simulation results represent the top 1 m of the soil column. The spatial pattern of soil carbon content is fairly well reproduced by our model and the simulated global total (1423 GtC) is somewhat lower than the estimate of Batjes (2008) (1549 GtC). Soil carbon inventories are underestimated in arctic and tropical wetlands as peat accumulation is not simulated in LPJ. In contrast, soil carbon is generally overestimated in cold and dry regions as well as in permafrost soils. The latter can be explained by the crude representation of processes in frozen ground in our version of LPJ. Simulated soil carbon content agrees well with observation-based values in temperate and tropical regions which are most affected by ALCC. Jobbagy and Jackson (2000) estimate a global soil carbon inventory of 2344 GtC for the top 3 m and 1502 GtC in the top 1 m. We consider only the top 1 m since soil carbon losses due to agricultural management below 1 m are not supported by field measurements (Guo and Gifford, 2002).

Our model has a tendency to overestimate forest biomass in most regions, when comparing results with 145 point measurements given by Luysaert et al. (2007). Simulated global

Table 1. Primary carbon emissions from ALCC (in GtC). Comparison of this study's four scenarios (HY, H2, OS, LIN) with published results. "present" refers to 2004 AD if not indicated otherwise; "industrial" refers to the period between 1850 and "present", unless indicated differently. ^aHYDE data, shifting cultivation between 23° N and 23° S; ^bHYDE data, no shifting cultivation.

	until 1850 AD	industrial	until present
HY	69	164	233
H2	105	142	247
OS	70	165	235
LIN	231	3	234
<i>no harvest/tillage</i>			
HY	50	127	177
H2	74	109	183
OS	47	128	175
LIN	153	0	153
<i>harvest after Shevliakova et al. (2009)</i>			
HY	73	172	245
DeFries et al. (1999)	48–57	125–151	182–199 (1987)
Houghton (2003)		156 (1850–2000)	
Strassmann et al. (2008)	94	187	284
Olofsson and Hickler (2008)	114	148	262 (1990)
Pongratz et al. (2009b)	63	108	171 (2000)
Shevliakova et al. (2009) ^a		240 (1700–2000)	
Shevliakova et al. (2009) ^b		161 (1700–2000)	
Kaplan et al. (2011)	325–357		
Kaplan et al. (2011), HYDE data	137–189		

total vegetation carbon is 980 GtC; this is slightly above the range of other DGVM simulations (557–923 GtC) (Kucharik et al., 2000; Krinner et al., 2005; Sitch et al., 2003). Although the PFT-parameter changes mentioned in Sect. 2.2 result in lower biomass densities in boreal regions, simulated values are still high, particularly in boreal regions. The same applies for temperate forests, where preindustrial ALCC was most prominent. In conclusion, the overestimation of forest biomass implies that direct carbon emissions from forest conversion are likely overestimated for a given ALCC scenario.

ALCC-related carbon emissions result from the reduction of carbon storage in ecosystems due to the clearing of forests and soil carbon losses due to an imbalance of carbon inputs and soil respiration as well as due to top soil erosion. Given the large size of the soil carbon inventory and the long time scale of interest, an understanding of the fate of soil carbon is key to assessing the human impact on the carbon cycle. The cultivation of cropland soils is associated with enhanced oxidation of soil organic matter due to tillage and a decreased litter input due to harvest and the removal of biomass from the field. A wide array of review studies report an average reduction in soil carbon by ~30% (Davidson and Ackerman, 1993; Amundson, 2001; Murty et al., 2002; Guo and Gifford, 2002; Ogle et al., 2005) when forest is converted to cropland. Smaller reductions (22%) are found when results are adjusted for changes in bulk density (Murty et al., 2002).

Largest carbon losses are found in the top 30 cm (Davidson and Ackerman, 1993; Murty et al., 2002; Guo and Gifford, 2002). In a literature review, Murty et al. (2002) report an average loss of $45 \pm 6\%$ in the top 15 cm, but only $19 \pm 6\%$ for soils sampled to more than 45 cm depth. Guo and Gifford (2002) report no changes in soils below 60 cm for forest to crop conversion.

Soil carbon exhibits no consistent response when forests are converted to pastures (Lugo and Brown, 1993; Murty et al., 2002; Guo and Gifford, 2002). Increased, as well as decreased storage is reported from individual site studies. In their reviews, Guo and Gifford (2002) report an increase of 7 to 13% for soils of less than 100 cm depth and no changes for greater depths, while Murty et al. (2002) report an average increase of $6 \pm 7\%$. The response of soil carbon on pastures depends on management and the history of land use (Lugo and Brown, 1993; Fearnside and Barbosa, 1998). Overgrazing can lead to a large decrease in soil carbon stocks locally (Abril and Bucher, 2001). 7.7% of the world's grasslands are classified as overgrazed, of which less than 10% are considered to be severely or extremely overgrazed (Conant and Paustian, 2002).

The paradigm of a rapid loss of soil carbon within the first years after land conversion and an establishment of a new equilibrium within decades is advocated by various authors (Amundson, 2001; McLauchlan, 2006). The millennial-scale effects of soil cultivation are less clear and strongly depend

on agricultural management. Examples where soil carbon was depleted even centuries after cessation of cultivation contrast with cases where organic amendments, charcoal additions or anaerobic soil conditions in paddy fields have lead to elevated soil carbon (Wu et al., 2003; McLauchlan, 2006). Unfortunately, such information is not available on the spatio-temporal scale of the present study.

Soil erosion affects soil carbon stocks locally. Although the total amount of mobilized carbon due to agricultural activity can be large, Quinton et al. (2010) suggest that a relatively small fraction is actually lost to the atmosphere and that most of the mobilized carbon is deposited downslope or buried in lakes, streams or wetlands. There, its decomposition is dramatically slowed (Amundson, 2001). Erosion processes may be implicitly included in review studies assessing soil carbon losses on cultivated land. For example, Wu et al. (2003) analyze over 30 000 soil profiles and compare soil stocks between cultivated and pristine lands in China.

The model applied here yields a reduction in soil carbon in the top 1 m of order 20% after conversion of natural vegetation to cropland and of 43% after conversion of natural grasslands to cropland, broadly consistent with the mentioned review studies. About half of the losses are attained in the first 10 yr after conversion and a final equilibrium is attained on a millennial time scale. Differences in NPP before and after conversion affect local responses. The model tends to underestimate losses in tropical and dry climates but is compatible with observations in temperate regions (Ogle et al., 2005). Modelled soil carbon increases after conversion from forests to pasture largely offset losses on croplands and overall, simulated changes in global soil carbon from ALCC are small.

Using the alternative harvest scheme, conversion to croplands leads to an accumulation of carbon in the tropics, while temperate and boreal regions respond similarly as in the standard treatment. The simulated response in the tropics disagrees with findings of Ogle et al. (2005), who report respective reductions by 42%.

The fact that peat and permafrost regions are not explicitly simulated is expected to have only a small effect on the simulated ALCC-related carbon emissions, as the overlap of preindustrial land use areas with peatlands and permafrost soils is relatively small on the global scale.

Next, published estimates of land use emissions are compared with results from this study. For the 1980s and 1990s, simulated average primary ALCC emissions based on the HYDE data are 1.12 and 0.95 GtC yr⁻¹, respectively. This is lower than the “bookkeeping” estimates of Houghton (2003) ($\sim 2.2 \pm 0.6$ GtC yr⁻¹), but in the range of estimates from Achard et al. (2002); DeFries et al. (1999); Strassmann et al. (2008); Shevliakova et al. (2009). Various estimates for cumulative emissions exist for the industrial period. Our estimate of 164 GtC for HY is close to results of DeFries et al. (1999); Houghton (2003); Olofsson and Hickler (2008) (see Table 1). Differences to Strassmann et al. (2008) can be explained by improved parameter values and the resulting

smaller biomass density in boreal forests, higher biomass density on grasslands and the inclusion of a management parametrization. In Pongratz et al. (2009b), lower values can partly be explained with differences in the ALCC data set where cropland is allowed to expand onto pasture (Houghton, 2010) and with the neglect of reduced inputs to the soil pool due to harvest. Cumulative primary emissions of 192 between 1700 and 2000 agree with the range of Shevliakova et al. (2009) (161 to 210 GtC) for their scenarios without shifting cultivation and forest management. An additional 60 to 80 GtC might have been emitted in response to shifting cultivation and forest management over the industrial period (Shevliakova et al., 2009) – factors not explicitly considered in our study.

Land use emission for the period before 1850 and for the HY scenario are with 69 GtC well within the range of most other studies (Table 1). Studies on historical ALCC are often based on the HYDE data (Strassmann et al., 2008) or related products (Shevliakova et al., 2009; Pongratz et al., 2009b), where land use area scales with population numbers.

Recently, Kaplan et al. (2011) presented an upward-revised land use scenario. Their high estimate (~ 150 GtC at 1 AD) is bracketed by our scenario range of 14–195 GtC until 1 AD. In addition, Kaplan et al. (2011) provide results for the HYDE 3.1 scenario that are directly comparable to the present study. They simulate much larger ALCC-related carbon emission per unit area converted than previous studies and the present one. Kaplan et al. (2011) do not discuss why they yield much higher emissions per unit area and results are only provided up to 1850 AD. Differences may arise from a number of reasons, such as different harvesting schemes, a different spatial resolution of the model, differences in the distribution of soil carbon, or differences in process formulations between models. In the model of Kaplan et al. (2011), the soil pool is adjusted upwards by roughly 50% to represent the top 3 m of the soil column, while most other studies consider soil pools for the top 1 m. In addition, no distinction is made between croplands and pastures and 100% of aboveground biomass is harvested annually on all agricultural land. This leads to a depletion of soil carbon pools by roughly $\sim 30\%$ not only in cropland soils but also on pastures and in the entire soil column of managed soils. A global average loss of 30% for the top 3 m on all cultivated land is not supported by available review studies (Davidson and Ackerman, 1993; Amundson, 2001; Murty et al., 2002; Guo and Gifford, 2002; Wu et al., 2003; Ogle et al., 2005; McLauchlan, 2006). As discussed above, reductions in soil carbon appear to be restricted to the upper soil layers and, on average, soil stocks even increase slightly after conversion from forest to pasture (Murty et al., 2002; Guo and Gifford, 2002).

Table 2. Global mean land area per person (LAP, in ha./pers.). The values for the four scenarios are derived by dividing the global land use area of the scenario and the global population as given in Klein Goldewijk (2001); Klein Goldewijk and van Drecht (2006). Note, that values of Lanly (1985); Ramankutty et al. (2002); Gregg (1988) given in the lower part of the table do not represent a global mean, but represent a specific agricultural system.

	1000 BC	1000 AD	1850 AD
HY	1.3	1.0	1.1
H2	2.5	2.1	1.6
OS	9.5	3.3	1.1
LIN	32	15	3.8
Ramankutty et al. (2002)	0.35–0.07 (per cap. cropland decrease in 20th cent.)		
Ruddiman and Ellis (2009)	4 ± 2 (“per-capita land use” at 5000 BC)		
Ruddiman and Ellis (2009)	0.4 ± 0.2 (before industrialisation)		
Gregg (1988)	4 (European late-neolithic settlement)		
Kaplan et al. (2011)	5.5–8.2 at 6000 BC		
Kaplan et al. (2011)	2.5–0.5 at 1850 AD		

4.2 ALCC reconstructions

Reconstructing land conversion in the Holocene remains challenging and the currently available datasets neglect potentially important effects of human activities on biomass density such as time varying land demand per person, or management practices such as shifting cultivation and wood harvesting. We address the uncertainty of Holocene ALCC reconstructions using three additional, idealized scenarios with larger preindustrial ALCC than in HY. The modern ALCC is the same in all scenarios. The four scenarios span a wide range from supposedly low (HY) to a purely schematic upper limit scenario (LIN) with respect to the magnitude and global extent of preindustrial ALCC. In the overshoot scenario (OS), technological change is assumed to lead to a decline in LAP over the centuries and, in combination with population declines after the Medieval age, to a drop in the global land use area. After 1700 AD, ALCC in OS rises in accordance with the HY scenario. The scenario range is designed to cover discrepancies among previously published reconstructions (Klein Goldewijk, 2001; Klein Goldewijk and van Drecht, 2006; Olofsson and Hickler, 2008; Pongratz et al., 2008; Kaplan et al., 2009) and hypotheses (Ruddiman and Ellis, 2009) and addresses the resilience of carbon stocks after land abandonment. Applying global scaling factors neglects the spatially differentiated evolution of agricultural practices. However, no global dataset exists that differentiates such practices throughout the Holocene. This leads to uncertainty in associated regional carbon fluxes from ALCC, as they depend strongly on the location of land conversion and the simulated carbon stocks in the respective grid cell.

It is undisputed that shifting cultivation, where forest clearings are (partly) balanced by regrowth on abandoned plots, has a qualitatively different (gross) effect on the local scale carbon budget than permanent agriculture (Brady, 1996; Olofsson and Hickler, 2008; Shevliakova et al., 2009).

Here we are interested in the net effect on CO₂ emissions induced by clearings and parallel regrowth. Over a large area where cultivated and abandoned plots coexist, mean biomass density is generally reduced as compared to an area where cultivation is restricted to a small and permanent area and the rest is left unaffected by forest clearings. For the preindustrial period, Kaplan et al. (2011) suggest an enhancement of cumulative emissions by about 15%.

The spread and the typical rotation length of non-permanent agriculture throughout the past millennia is highly uncertain and subject to ongoing debates (Williams, 2003; Mazoyer and Roudart, 2006) and simplifying assumptions even have to be made for the last three centuries (Hurt et al., 2006). Therefore, we argue that for the scope of the present study, the net effect of shifting cultivation can be adequately captured by a simple scaling of permanent land use areas. This in turn leads to accordingly higher cumulative emissions (see Table 1). Scenario H2 where preindustrial land use areas are 100% higher than in HY thus accounts for higher emissions from non-permanent agriculture. In brief, including shifting cultivation in the model is not expected to narrow uncertainties as global data on the extent in space and time, as well as on the rotation length is lacking.

4.3 Land Area per Person (LAP)

Next, we address the consistency of a scenario by comparing the implied global LAP with values proposed in the literature. Implied global mean LAP in 2000 AD is 0.80 ha/pers. according to the HYDE 3.1 data set (Goldewijk, 2001). LAP values at 1000 BC range from 1.3 and 2.5 in HY and H2, respectively to 32 ha/pers. in LIN (see Table 2). While the HY value is considerably lower than estimates proposed by other authors, values for LIN are incompatibly larger than published estimates (about 4 ha/pers. for neolithic agricultural systems). This also represents too large of an agricultural

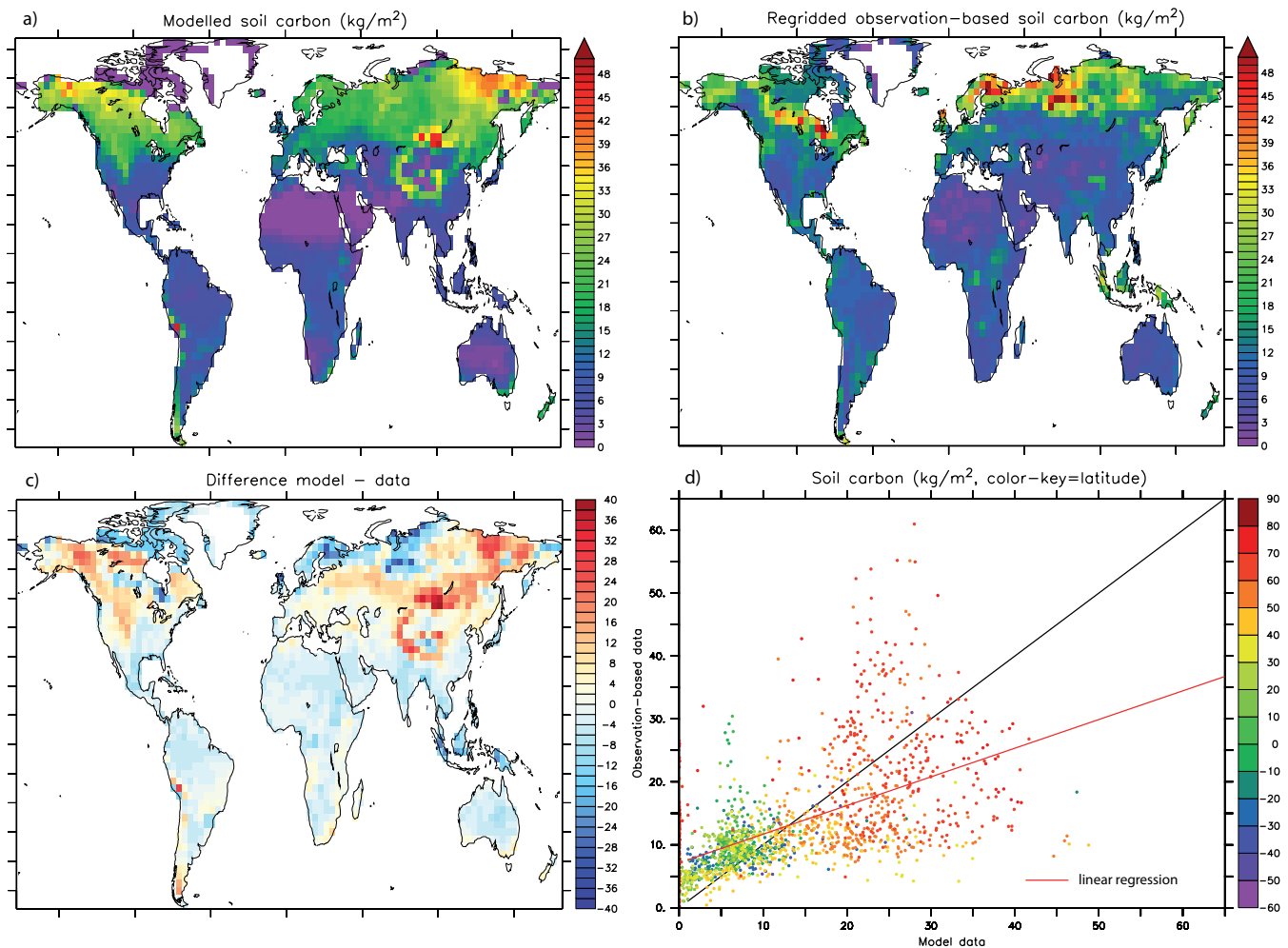


Fig. 5. Comparison of simulated soil carbon inventories with observation-based estimates for the top metre of the soil column. (a): modeled soil carbon inventory; (b): observed soil carbon inventory from Batjes (2008). The ISRIC map is regridded to the LPJ model grid; (c): difference: model minus observations; (d): modeled versus observed soil carbon inventory. The colour key depicts latitude of the respective measurement site.

area even when taking into account that global population estimates for the time before 1000 AD differ by a factor of up to 2 (Pongratz et al., 2008).

The concept of assessing a global mean LAP is rather crude. Global mean LAP does not necessarily represent the LAP in a certain agricultural system. The fact that the share of farming people was zero at around 12 kyr BP and continuously increased throughout the first half of the Holocene (Lemmen, 2009) implies that total agricultural land is to be divided by the *agricultural* population only, which is smaller than total population in this period. This in turn increases global mean LAP numbers considerably and make the values for LIN seem even more unrealistic. However, a large global extent of anthropogenically deforested areas at low global population numbers may be the result of extensive anthropogenic fires.

4.4 Residual sink test

An analysis of the budget of atmospheric CO₂ over the last millennium (Fig. 4) is used to further constrain the scenario space. Although, we technically considered the CO₂ budget only in a so-called single deconvolution, it is noted that analyses that consider both the evolution of CO₂ and of its stable carbon isotope ¹³C yield very similar results for net atmosphere-ocean and atmosphere land fluxes for the last millennium (Joos et al., 1999; Trudinger et al., 2002). The general pattern of a small residual, non-ALCC related terrestrial flux between 1000 AD and the mid 20th century and a significantly increasing terrestrial sink flux thereafter can be expected from the response of the land biosphere to changing environmental conditions (from a near-equilibrium state to increasing CO₂, nitrogen deposition, climatic change

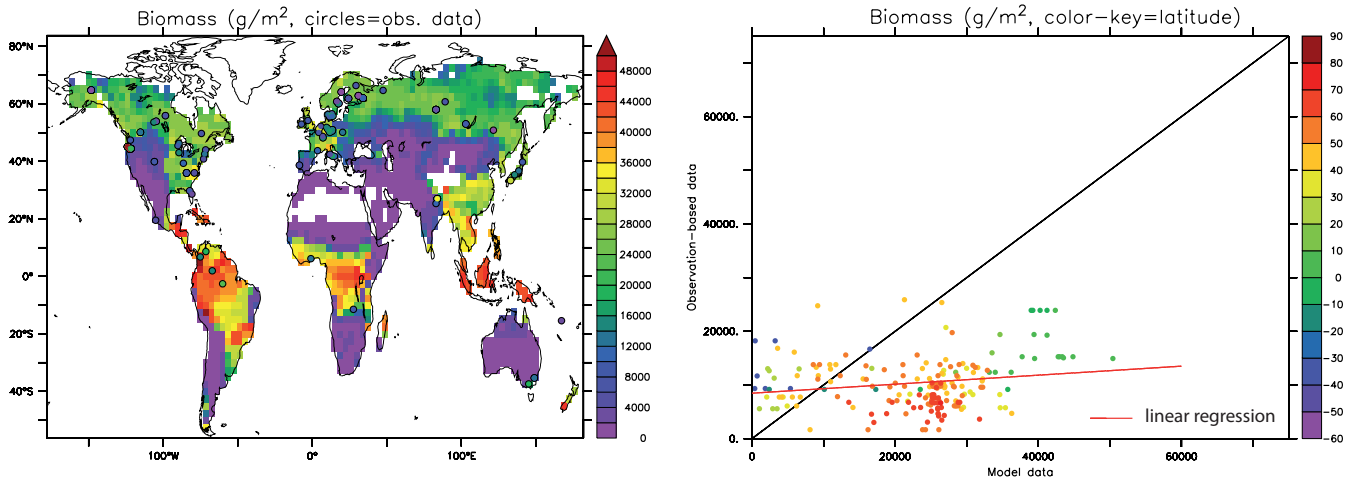


Fig. 6. Comparison of simulated forest biomass inventories with observation-based estimates. Left: modelled forest biomass inventory. The colour in circles represents observed biomass inventory at the measurement site from Luyssaert et al. (2007). Right: modeled versus observed forest biomass inventory. Observations are regridded to the model grid. The colour key depicts latitude of the respective measurement site.

and more recent vegetation regrowth, e.g. due to woody encroachment and fire prevention, not accounted for in ALCC data). HY, H2 and OS are broadly consistent with this temporal pattern and the budget of CO₂ (and implicitly ¹³CO₂) is roughly closed before 1880 AD. An implied sink of about 30 GtC between 1880 and 1940 AD may be interpreted as an indication that the share of pre- versus post-1850 AD ALCC is underestimated by the respective scenarios. In contrast, LIN suggests a large and unexplained terrestrial (not ALCC-related) release of ~70 GtC between 1700 and 1930 AD.

The mean residual sink fluxes in the 1980s and 1990s is -1.7 and -2.1 (-1.3 and -1.6) GtC yr⁻¹ in HY (H2). This is in the range given by Denman et al. (2007), namely -3.8 to -0.3 GtC yr⁻¹ for the 1980s and -4.3 to -0.9 GtC yr⁻¹ for the 1990s. A recently published estimate of the land sink flux is in the range of -0.9 to -1.36 GtC yr⁻¹ between 1989 and 2003 (Sarmiento et al., 2010). For a discussion on the variations of the land sink in the twentieth century, we refer to Strassmann et al. (2008).

The discussion in Sects. 4.2, 4.3 and 4.4 indicates that the wide scenario range applied implicitly accounts for uncertainties related to preindustrial management practices or the modelled carbon inventories in LPJ.

4.5 Timing and rate of emissions and implications for today's carbon budget

The scenarios are identical with respect to the land use areas at 10 000 BC, when sedentary agriculture was basically non-existent, and the land use areas in 2005 AD as constrained by satellite observations and surveys. This implies differences in the *timing* and the *rate* of ALCC-related carbon emissions, whereas cumulative net emissions converge to roughly the

same value by today. The various scenarios imply differences in the airborne fraction, the atmospheric CO₂ increase, and in the split of emission between periods.

The simulated airborne fraction of primary ALCC emissions for HY (28.6%) by year 2000 AD (see Fig. 3) is similar to the value (29%) in Pongratz et al. (2009b). Results based on the HYDE reconstruction suggest a split of 30 vs. 70% for pre-1850 vs. post-1850 primary emissions. Olofsson and Hickler (2008), who explicitly account for the marginal but widespread impact of shifting cultivation and longer fallow periods of croplands in earlier agricultural systems, suggest a much higher share of pre-1850 emissions (43%). This corresponds to the respective split in H2.

The split of emissions has important consequences for the CO₂ increase and residual sink flux. The standard scenario (HY) is associated with the highest CO₂ increase and airborne fraction by today. Doubling agricultural areas in 1700 AD (H2 scenario) yields a reduction of the CO₂ increase since 1850 AD by 13% relative to the standard scenario. The comparatively low preindustrial anthropogenic ALCC assumed in the HYDE data in turn implies large land use area changes over the industrial period. The discrepancies in ALCC reconstructions for the early industrial era (Kaplan et al., 2009, 2011; Gaillard et al., 2010) and the considerations discussed above, might point to a tendency of HYDE-based simulations to overestimate the ALCC-induced CO₂ increase over the last centuries.

The difference between the residual sink fluxes of HY and H2 increases from less than 0.1 GtC yr⁻¹ before 1900 AD to 0.5 GtC yr⁻¹ at present. This difference, which stems from different ALCC reconstructions, is much smaller than the total uncertainty of the residual sink flux (range: -4.3 to -0.9 GtC yr⁻¹) as given by Denman et al. (2007). Still, it

leaves a considerable uncertainty in this flux and prevents us from drawing further conclusions about the absolute magnitude of this sink. However, our results suggest that an upward revision of the ratio between preindustrial versus industrial ALCC as in the H2 scenario tend to reduce the modern residual terrestrial sink flux by $\sim 0.5 \text{ GtC yr}^{-1}$. This may help to reconcile the modern carbon budget as it appears difficult to explain current upper bound estimates of the residual sink flux mechanistically and their consistency with bottom-up estimates of land carbon fluxes (Denman et al., 2007).

4.6 Atmospheric CO₂ and radiative forcing during the last millennium and the Holocene

The contribution of ALCC to the last millennium CO₂ evolution is overall about 5 (8) ppm for the period 1000 to 1850 AD in the HY (H2) scenarios. In OS, the CO₂ rise between 1000 and 1850 AD was 4 ppm. The result of HY agrees with numbers reported for the “best-guess” scenario of Pongratz et al. (2009b). The ALCC related signal in atmospheric CO₂ is relevant when it comes to explain the weak CO₂ trends during the last millennium or to infer carbon cycle-warming feedbacks from reconstructed CO₂ and temperature (Gerber et al., 2003; Frank et al., 2010). The simulated interannual variability (IAV) range of atmospheric CO₂ is about ± 1.5 ppm and results directly from the IAV of the prescribed climatology. In scenario HY, atmospheric CO₂ clearly rises beyond this range after late Medieval times. After 1500 AD, the ALCC-related deviation from the natural IAV is striking. This corresponds to the finding of Pongratz et al. (2009b) and Jungclaus et al. (2010), who simulated intrinsic IAV of the coupled climate-carbon cycle system. Postulating an extent of land use areas that is twice as high as in the HY scenario is not sufficient to explain an atmospheric signal of more than 2 ppm before the Medieval period (see H2).

Ice core measurements of atmospheric CO₂ reveal a rise of ~ 20 ppm between 7 and 2 kyr BP. None of the scenarios reproduces the timing and amplitude of this increase. However, scenarios representing intensive early ALCC may explain part of it. In OS, where average LAP is 9.5 ha/pers. before 1000 BC, atmospheric CO₂ rises beyond its simulated interannual variability at 3000 BC but increases only by 3.5 ppm until 1 AD. Even in the extreme LIN scenario and without considering a potential CO₂ fertilization, atmospheric CO₂ increased by less than 8 ppm over the past 8 kyr. Allocating ALCC earlier in time causes a smaller CO₂ increase in the atmosphere as the ocean-sediment system has more time to absorb excess CO₂. The CO₂-fertilisation feedback reduces primary emissions by about 20–30%, depending on level of atmospheric CO₂ (see Fig. 3). Simulations with suppressed CO₂ fertilization yield accordingly higher atmospheric CO₂ levels (thin lines in Fig. 2, lower panel.)

The proposal that human activities are the primary driver for the late Holocene CO₂ increase is also difficult to recon-

cile with the timing of population growth and the temporal evolution of ALCC. Atmospheric CO₂ increases by 20 ppm between 7 and 2 kyr BP. Then, the CO₂ concentration essentially stabilizes and remains within a few ppm until the Maunder Minimum and the onset of the industrial period. If early agricultural activities would have indeed caused a CO₂ increase of 10 to 20 ppm between 7 and 2 kyr BP, one would expect that, with further population growth and expansion of civilizations, agricultural activities would at least cause a continuation of the CO₂ rise. While the timing of the late Holocene CO₂ increase appears inconsistent with anthropogenic forcing, natural processes such as ocean-sediment compensation of terrestrial carbon uptake during the transition and the early Holocene are consistent with the timing of the Holocene CO₂ evolution (e.g., Elsig et al., 2009; Joos et al., 2004).

The radiative forcing related to an increase in CO₂ of 3.5 ppm as found for the scenario with the highest cumulative emissions (OS) at 1 AD is 0.07 Wm^{-2} (see Myhre et al., 1998). An additional 0.1 Wm^{-2} forcing is computed under the extreme assumptions that all the Holocene CH₄ and N₂O changes are related to ALCC. Together these forcings imply a warming of merely 0.10 to 0.24 °C (for a nominal climate sensitivity of 2 to 4.5 °C for doubling CO₂) and a carbon cycle-warming feedback on the order of 1 ppm using median carbon cycle-climate sensitivities from Frank et al. (2010). The pronounced albedo increase of deforestation in the mid-latitudes (Betts et al., 2007) counteracts these biogeochemical forcings by as much as -0.2 Wm^{-2} for the present-day ALCC (IPCC, 2007) and by about -0.05 Wm^{-2} for the pre-1800 AD state (Pongratz et al., 2009a). A recent study (Pongratz et al., 2010) finds the warming biogeochemical forcing of ALCC to dominate the cooling biogeophysical forcing on the global scale. It is concluded that no significant human impact on global temperatures can be detected until the beginning of the industrial era when the ALCC-related CO₂ increase rose beyond 5–6 ppm (Pongratz et al., 2009a). In light of the new simulations presented herein, this conclusion appears to be valid for the entire preindustrial Holocene even when taken into account the large uncertainties for cumulative ALCC-related carbon emissions.

A number of natural processes have been invoked to explain the Holocene CO₂ and $\delta^{13}\text{C}$ evolution (Indermühle et al., 1999; Elsig et al., 2009; Joos et al., 2004; Kleinen et al., 2010; Ridgwell et al., 2003; Broecker et al., 2001; Brovkin et al., 2002, 2008; Schurgers et al., 2006). These include terrestrial uptake and release, ocean sediment compensation of terrestrial carbon uptake during the transition and the early Holocene, changes in coral reef growth, or changes in sea surface temperature affecting the solubility of CO₂ in water. Available studies suggest that a combination of natural processes is consistent both in magnitude and timing with the reconstructed Holocene CO₂ evolution. However, available proxy evidence is limited and it remains difficult to exactly quantify the contribution by individual mechanisms.

Atmospheric $\delta^{13}\text{C}$ data suggest that changes in the organic carbon stocks on land contributed significantly to the CO₂ changes over the past 11 kyr (Elsig et al., 2009). It is currently unclear to which extent individual terrestrial mechanisms and land regions have contributed to the CO₂ and $\delta^{13}\text{C}$ evolution. More work is needed to disentangle the contributions from peat- and wetlands, permafrost regions, from forest regrowth in the wake of ice sheet retreat and milder climatic conditions, from dieback of vegetation due to flooding by sea level rise or from vegetation changes associated with changes in the monsoon system. A particular effort is needed to represent the net exchange of carbon between the atmosphere and wetlands, peatlands and permafrost regions in models. A complicating factor is the millennial adjustment time scale associated with ocean-sediment processes. Reorganizations of the carbon cycle during the glacial-interglacial transitions can also have implications for the Holocene CO₂ and $\delta^{13}\text{C}$ evolution (Tschumi et al., 2010). Here, a bottom-up approach is used to quantify the possible contribution from human activities. The model results suggest that human activities may have contributed a few ppm to the 20 ppm CO₂ rise between 7 and 2 kyr BP, implying that natural mechanisms dominate.

5 Conclusions

A wide range of land use scenarios has been applied in the BernCC coupled climate-carbon cycle model to simulate the potential human impact on carbon emissions and atmospheric CO₂. Carbon emissions arising from preindustrial anthropogenic land cover changes have not been sufficient to explain the timing and amplitude of the reconstructed increase in atmospheric CO₂ over the Holocene. This conclusion appears robust with regard to uncertainties in ALCC-induced carbon losses, uncertainties in the ALCC reconstructions and the strength of CO₂-fertilization. We have demonstrated that placing ALCC emissions at an earlier time leaves the ocean more time to absorb excessive CO₂ and results in a smaller atmospheric CO₂ signal. Natural processes such as changes in the ocean calcium carbonate cycle and natural terrestrial carbon stock changes are required to explain the mid to late Holocene CO₂ increase (Elsig et al., 2009; Kleinen et al., 2010).

This study does not tackle a potentially profound early human impact on local scale environmental conditions by alterations of the natural vegetation cover and cultivation of the soils. Improved global data sets for preindustrial ALCC and explicitly simulating different land management practices (spatio-temporal evolution of LAP, shifting cultivation, distinction between croplands and pastures, wood harvesting, wet rice agriculture etc.) will be crucial for a refined assessment of the human impact on the climate, the contemporary residual terrestrial sink and to address the human impact on the methane cycle.

Acknowledgements. We thank R. Spahni, J. Kaplan, K. Krumhardt, D. Frank, M. Steinacher, H. Fischer, and the reviewers for comments, support, and language revisions. We appreciate support by the Swiss National Science Foundation through the National Centre of Competence in Research (NCCR) Climate and by the European Commission through the FP7 project Past4Future (grant no. 243908).

Edited by: V. Brovkin

References

- Abril, A. and Bucher, E. H.: Overgrazing and soil carbon dynamics in the western Chaco of Argentina, *Appl. Soil Ecol.*, 16, 243–249, doi:10.1016/S0929-1393(00)00122-0, 2001.
- Achard, F., Eva, H. D., Stibig, H. J., Mayaux, P., Gallego, J., Richards, T., and Malingreau, J. P.: Determination of deforestation rates of the world's humid tropical forests, *Science*, 297, 999–1002, 2002.
- Amundson, R.: The carbon budget in soils, *Annual Review of Earth and Planetary Sciences*, 29, 535–562, doi:10.1146/annurev.earth.29.1.535, 2001.
- Archer, D., Keshgi, H., and Maier-Reimer, E.: Multiple timescales for neutralization of fossil fuel CO₂, *Geophys. Res. Lett.*, 24, 405–408, 1997.
- Batjes, N.: ISRIC-WISE Harmonized Global Soil Profile Dataset (Ver. 3.1), Tech. rep., ISRIC – World Soil Information, Wageningen, www.isric.org/isric/Webdocs/docs/ISRIC_report_2008_02.pdf, 2008.
- Berger, A.: Long-term variations of daily insolation and Quaternary climatic changes, *J. Atmos. Sci.*, 35, 2362–2367, 1978.
- Betts, R. A., Falloon, P. D., Goldewijk, K. K., and Ramankutty, N.: Biogeophysical effects of land use on climate: Model simulations of radiative forcing and large-scale temperature change, *Agr. Forest Meteorol.*, 142, 216–233, 2007.
- Bonan, G. B.: Forests and Climate Change: Forcings, Feedbacks, and the Climate Benefits of Forests, *Science*, 320, 1444–1449, doi:10.1126/science.1155121, 2008.
- Brady, N. C.: Alternatives to slash and burn: a global imperative, *Agr. Ecosyst. Environ.*, 58, 3–11, 1996.
- Broecker, W. S., Lynch-Stieglitz, J., Clark, E., Hajdas, I., and Bonani, G.: What caused the atmosphere's CO₂ content to rise during the last 8000 years?, *Geochem. Geophys. Geosy.*, 2, 1062–1074, doi:10.1029/2001GB000177, 2001.
- Brovkin, V., Bendtsen, J., Claussen, M., Ganopolski, A., Kubatzki, C., Petoukhov, V., and Andreev, A.: Carbon cycle, vegetation, and climate dynamics in the Holocene: Experiments with the CLIMBER-2 model, *Global Biogeochem. Cy.*, 16, 1139–1159, 2002.
- Brovkin, V., Claussen, M., Driesschaert, E., Fichet, T., Kicklighter, D., Loutre, M., Matthews, H., Ramankutty, N., Schaeffer, M., and Sokolov, A.: Biogeophysical effects of historical land cover changes simulated by six Earth system models of intermediate complexity, *Clim. Dynam.*, 26, 587–600, 2006.
- Brovkin, V., Kim, J.-H., Hofmann, M., and Schneider, R.: A lowering effect of reconstructed Holocene changes in sea surface temperatures on the atmospheric CO₂ concentration, *Global Biogeochem. Cy.*, 22, GB1016, doi:10.1029/2006GB002885, 2008.

- Bruno, M. and Joos, F.: Terrestrial carbon storage during the past 200 years: A Monte Carlo Analysis of CO₂ data from ice core and atmospheric measurements, *Global Biogeochem. Cy.*, 11, 111–124, 1997.
- Cao, L., Eby, M., Ridgwell, A., Caldeira, K., Archer, D., Ishida, A., Joos, F., Matsumoto, K., Mikolajewicz, U., Mouchet, A., Orr, J. C., Plattner, G.-K., Schlitzer, R., Tokos, K., Totterdell, I., Tschumi, T., Yamanaka, Y., and Yool, A.: The role of ocean transport in the uptake of anthropogenic CO₂, *Biogeosciences*, 6, 375–390, doi:10.5194/bg-6-375-2009, 2009.
- Conant, R. T. and Paustian, K.: Potential soil carbon sequestration in overgrazed grassland ecosystems, *Global Biogeochem. Cy.*, 16, 1143–1142, doi:10.1029/2001GB001661, 2002.
- Davidson, E. A. and Ackerman, I. L.: Changes in Soil Carbon Inventories Following Cultivation of Previously Untilled Soils, *Biogeochemistry*, 20, 161–193, 1993.
- DeFries, R. S., Field, C. B., Fung, I., Collatz, G. J., and Bounoua, L.: Combining satellite data and biogeochemical models to estimate global effects of human-induced land cover change on carbon emissions and primary productivity, *Global Biogeochem. Cy.*, 13, 803–815, 1999.
- Denman, K. L., Brasseur, G., Chidthaisong, A., Ciais, P., Cox, P., Dickinson, R. E., Hauglustaine, D., Heinze, C., Holland, E., Jacob, D., Lohmann, U., Ramachandran, S., da Silva Dias, P. L., Wofsy, S. C., and Zhang, X.: Chapter 7: Couplings Between Changes in the Climate System and Biogeochemistry, in: *Climate Change 2007: The Physical Science Basis. Contribution of Working Group I to the Fourth Assessment Report of the Intergovernmental Panel on Climate Change*, edited by: Solomon, S., Qin, D., Manning, M., Chen, Z., Marquis, M., Averyt, K., Tignor, M., and Miller, H., Cambridge Univ. Press, United Kingdom and New York, NY, USA, 2007.
- Diamond, J.: Evolution, consequences and future of plant and animal domestication, *Nature*, 418, 700–707, 2002.
- Elsig, J., Schmitt, J., Leuenberger, D., Schneider, R., Eyer, M., Leuenberger, M., Joos, F., Fischer, H., and Stocker, T. F.: Stable isotope constraints on Holocene carbon cycle changes from an Antarctic ice core, *Nature*, 461, 507–510, 2009.
- Etheridge, D. M., Steele, L. P., Langenfelds, R. L., Francey, R. J., Barnola, J., and Morgan, V. I.: Natural and anthropogenic changes in atmospheric CO₂ over the last 1000 years from air in Antarctic ice and firn, *J. Geophys. Res.*, 101, 4115–4128, doi:10.1029/95JD03410, 1996.
- Fearnside, P. M. and Barbosa, R. I.: Soil carbon changes from conversion of forest to pasture in Brazilian Amazonia, *Forest Ecol. Manag.*, 108, 147–166, doi:10.1016/S0378-1127(98)00222-9, 1998.
- Francey, R. J., Allison, C. E., Etheridge, D. M., Trudinger, C. M., Enting, I. G., Leuenberger, M., Langenfelds, R. L., Michel, E., and Steele, L. P.: A 1000-year high precision record of $\delta^{13}\text{C}$ in atmospheric CO₂, *Tellus B*, 51, 170–193, doi:10.1034/j.1600-0889.1999.t01-1, 1999.
- Frank, D. C., Esper, J., Raible, C. C., Büntgen, U., Trouet, V., Stocker, B., and Joos, F.: Ensemble reconstruction constraints on the global carbon cycle sensitivity to climate, *Nature*, 463, 527–530, doi:10.1038/nature08769, 2010.
- Gaillard, M.-J., Sugita, S., Mazier, F., Trondman, A.-K., Broström, A., Hickler, T., Kaplan, J. O., Kjellström, E., Kokfelt, U., Kuneš, P., Lemmen, C., Miller, P., Olofsson, J., Poska, A., Rundgren, M., Smith, B., Strandberg, G., Fyfe, R., Nielsen, A. B., Aalenius, T., Balakauskas, L., Barnekow, L., Birks, H. J. B., Bjune, A., Björkman, L., Giesecke, T., Hjelle, K., Kalnina, L., Kangur, M., van der Knaap, W. O., Koff, T., Lagerås, P., Latałowa, M., Leydet, M., Lechterbeck, J., Lindbladh, M., Odgaard, B., Peglar, S., Segerström, U., von Stedingk, H., and Seppä, H.: Holocene land-cover reconstructions for studies on land cover-climate feedbacks, *Clim. Past*, 6, 483–499, doi:10.5194/cp-6-483-2010, 2010.
- Gerber, S., Joos, F., Brügger, P., Stocker, T. F., Mann, M. E., Sitch, S., and Scholze, M.: Constraining temperature variations over the last millennium by comparing simulated and observed atmospheric CO₂, *Clim. Dynam.*, 20, 281–299, doi:10.1007/s00382-002-0270-8, 2003.
- Goldewijk, K. K.: Estimating global land use change over the past 300 years: the HYDE database, *Global Biogeochem. Cy.*, 15, 417–434, 2001.
- Gregg, S. A.: Foragers and Farmers: Population Interaction and Agricultural Expansion in Prehistoric Europe, *Prehistoric Archaeology and Ecology Series*, The University of Chicago Press, 1988.
- Guo, L. B. and Gifford, R. M.: Soil carbon stocks and land use change: a meta analysis, *Glob. Change Biol.*, 8, 345–360, doi:10.1046/j.1354-1013.2002.00486.x, 2002.
- Houghton, R. A.: Revised estimates of the annual net flux of carbon to the atmosphere from changes in land use and land management 1850–2000, *Tellus*, 55B, 378–390, 2003.
- Houghton, R. A.: How well do we know the flux of CO₂ from land-use change, *Tellus B*, 62, 337–351, 2010.
- Houghton, R. A., Joos, F., and Asner, G. P.: The effects of land use and management on the global carbon cycle, in: *Land Change Science Observing, Monitoring and Understanding Trajectories of Change on the Earth's Surface*, edited by: Turner, I. I., Gutzman, G., Janetos, A. C., Justice, C. O., Moran, E. F., Mustard, J. F., Rindfuss, R. R., Skole, D., and Cochrane, M. A., 2004.
- Hurtt, G. C., Frolking, S., Fearon, M. G., Moore, B., Shevliakova, E., Malyshev, S., Pacala, S. W., and Houghton, R. A.: The underpinnings of land-use history: three centuries of global gridded land-use transitions, wood-harvest activity, and resulting secondary lands, *Glob. Change Biol.*, 12, 1208–1229, doi:10.1111/j.1365-2486.2006.01150.x, 2006.
- Indermühle, A., Stocker, T. F., Joos, F., Fischer, H., Smith, H. J., Wahlen, M., Deck, B., Mastroianni, D., Tschumi, J., Blunier, T. R., and Stauffer, B.: Holocene carbon-cycle dynamics based on CO₂ trapped in ice at Taylor Dome, Antarctica, *Nature*, 398, 121–126, doi:10.1038/18158, 1999.
- IPCC: Summary for Policymakers, in: *Climate Change 2007: The Physical Science Basis. Contribution of Working Group I to the Fourth Assessment Report of the Intergovernmental Panel on Climate Change*, edited by: Solomon, S., Qin, D., Manning, M., Chen, Z., Marquis, M., Averyt, K., Tignor, M., and Miller, H., Cambridge Univ. Press, United Kingdom and New York, NY, USA, 2007.
- Jobbagy, E. G. and Jackson, R. B.: The Vertical Distribution of Soil Organic Carbon and Its Relation to Climate and Vegetation, *Ecol. Appl.*, 10, 423–436, doi:10.2307/2641104, 2000.
- Joos, F. and Bruno, M.: Long-term variability of the terrestrial and oceanic carbon sinks and the budgets of the carbon isotopes ¹³C and ¹⁴C, *Global Biogeochem. Cy.*, 12, 277–295, 1998.

- Joos, F., Bruno, M., Fink, R., Stocker, T. F., Siegenthaler, U., Le Quééré, C., and Sarmiento, J. L.: An efficient and accurate representation of complex oceanic and biospheric models of anthropogenic carbon uptake, *Tellus*, 48B, 397–417, 1996.
- Joos, F., Meyer, R., Bruno, M., and Leuenberger, M.: The variability in the carbon sinks as reconstructed for the last 1000 years, *Geophys. Res. Lett.*, 26, 1437–1440, 1999.
- Joos, F., Prentice, I. C., Sitch, S., Meyer, R., Hooss, G., Plattner, G.-K., Gerber, S., and Hasselmann, K.: Global warming feedbacks on terrestrial carbon uptake under the Intergovernmental Panel on Climate Change (IPCC) emission scenarios, *Global Biogeochem. Cy.*, 15, 891–907, 2001.
- Joos, F., Gerber, S., Prentice, I. C., Otto-Bliesner, B. L., and Valdes, P. J.: Transient simulations of Holocene atmospheric carbon dioxide and terrestrial carbon since the Last Glacial Maximum, *Global Biogeochem. Cy.*, 18, 1–18, doi:10.1029/2003GB002156, 2004.
- Jungclaus, J. H., Lorenz, S. J., Timmreck, C., Reick, C. H., Brovkin, V., Six, K., Segsneider, J., Giorgetta, M. A., Crowley, T. J., Pongratz, J., Krivova, N. A., Vieira, L. E., Solanki, S. K., Klocke, D., Botzet, M., Esch, M., Gayler, V., Haak, H., Raddatz, T. J., Roeckner, E., Schnur, R., Widmann, H., Claussen, M., Stevens, B., and Marotzke, J.: Climate and carbon-cycle variability over the last millennium, *Clim. Past*, 6, 723–737, doi:10.5194/cp-6-723-2010, 2010.
- Kaplan, J., Krumhardt, K., and Zimmermann, N.: The prehistoric and preindustrial deforestation in Europe, *Quaternary Sci. Rev.*, 28, 3016–3034, 2009.
- Kaplan, J. O., Krumhardt, K. M., Ellis, E. C., Ruddiman, W. F., Lemmen, C., and Klein Goldewijk, K.: Holocene carbon emissions as a result of anthropogenic land cover change, *The Holocene*, doi:10.1177/0959683610386983, in press, 2011.
- Keeling, C. D. and Whorf, T. P.: Atmospheric CO₂ records from sites in the SIO air sampling network, in: *Trends: A Compendium of Data on Global Change, Carbon Dioxide Information Analysis Center, Oak Ridge National Laboratory, U.S. Department of Energy, Oak Ridge, Tenn., U.S.A.*, 2003.
- Keeling, R., Najjar, R. P., Bender, M. L., and Tans, P. P.: What atmospheric oxygen measurements can tell us about the global carbon cycle, *Global Biogeochem. Cy.*, 7, 37–67, 1993.
- Klein Goldewijk, K.: Estimating global land use change over the past 300 years: The HYDE Database, *Global Biogeochem. Cy.*, 15, 417–433, 2001.
- Klein Goldewijk, K. and van Drecht, G.: HYDE3: Current and historical population and land cover, in: *Integrated modelling of global environmental change. An overview of IMAGE 2.4.*, edited by: Bouwman, A. F., Kram, T., and Klein Goldewijk, K., Netherlands Environmental Assessment Agency (MNP), Bilthoven, The Netherlands, 2006.
- Kleinen, T., Brovkin, V., von Bloh, W., Archer, D., and Munhoven, G.: Holocene carbon cycle dynamics, *Geophys. Res. Lett.*, 37, L02705, doi:10.1029/2009GL041391, 2010.
- Krinner, G., Viovy, N., de Noblet-Ducoudré, N., Ogée, J., Polcher, J., Friedlingstein, P., Ciais, P., Sitch, S., and Prentice, C.: A dynamic global vegetation model for studies of the coupled atmosphere-biosphere system, *Global Biogeochem. Cy.*, 19, GB1015, doi:10.1029/2003GB002199, 2005.
- Kucharik, C. J., Foley, J. A., Delire, C., Fisher, V. A., Coe, M. T., Lenters, J. D., Young-Molling, C., and Ramankutty, N.: Testing the performance of a Dynamic Global Ecosystem Model: Water balance, carbon balance, and vegetation structure, *Global Biogeochem. Cy.*, 14, 795–825, 2000.
- Lanly, J.: Defining and measuring shifting cultivation, *Unasylva*, 37, 17–21, 1985.
- Leemans, R. and Cramer, W.: The IIASA climate database for land areas on a grid with 0.5° resolution, Research Report RR-91-18, Tech. rep., International Institute for Applied System Analysis, 1991.
- Lemmen, C.: World distribution of land cover changes during Pre- and Protohistoric Times and estimation of induced carbon releases, *Geomorphologie*, 4, 303–312, doi:10.5194/cpd-6-307-2010, 2009.
- Lugo, A. and Brown, S.: Management of tropical soils as sinks or sources of atmospheric carbon, *Plant Soil*, 149, 27–41, doi:10.1007/BF00010760, 1993.
- Lüthi, D., Floch, L. M., Bereiter, B., Blunier, T., Barnola, J. M., Siegenthaler, U., Raynaud, D., Jouzel, J., Fischer, H., Kawamura, K., and Stocker, T. F.: High-resolution carbon dioxide concentration record 650 000–800 000 years before present, *Nature*, 453, 379–382, 2008.
- Luyssaert, S., Inglisma, I., Jung, M., Richardson, A. D., Reichstein, M., Ppapale, D., Piao, S. L., Schulze, E.-D., Wingate, L., Matteucci, G., Aragao, L., Aubinet, M., Beer, C., Bernhofer, C., Black, K. G., Bonal, D., Bonnefond, J.-M., Chambers, J., Ciais, P., Cook, B., Davis, K. J., Dolman, A. J., Gielen, B., Goulden, M., Grace, J., Granier, A., Grelle, A., Griffis, T., Grünwald, T., Guidolotti, G., Hanson, P. J., Harding, R., Hollinger, D. Y., Hutrya, L. R., Kolar, P., Kruijft, B., Kutsch, W., Lagergren, F., Laurila, T., Law, B. E., Le Maire, G., Lindroth, A., Loustau, D., Malhi, Y., Mateus, J., Migliavacca, M., Misson, L., Montagnani, L., Moncrieff, J., Moors, E., Munger, J. W., Nikinmaa, E., Ollinger, S. V., Pita, G., Rebmann, C., Rouspard, O., Saigusa, N., Sanz, M. J., Seuffert, G., Sierra, C., Smith, M.-L., Tang, J., Valentini, R., Vesala, T., and Janssens, I. A.: CO₂ balance of boreal, temperate, and tropical forests derived from a global database, *Glob. Change Biol.*, 13, 2509–2537, 2007.
- MacDonald, G. M., Beilman, D. W., Kremenetski, K. V., Sheng, Y., Smith, L. C., and Velichko, A. A.: Rapid Early Development of Circumarctic Peatlands and Atmospheric CH₄ and CO₂ Variations, *Science*, 314, 285–288, doi:10.1126/science.1131722, 2006.
- Marland, G., Boden, T. A., and Andres, R. J.: Global, Regional, and National CO₂ Emissions, in: *Trends: A Compendium of Data on Global Change, Carbon Dioxide Information Analysis Center, Oak Ridge National Laboratory, U.S. Department of Energy, Oak Ridge, Tenn., U.S.A.*, 2006.
- Marlon, J. R., Bartlein, P. J., Carcaillet, C., Gavin, D. G., Harrison, S. P., Higuera, P. E., Joos, F., Power, M. J., and Prentice, I. C.: Climate and human influences on global biomass burning over the past two millennia, *Nat. Geosci.*, 2, 307–307, 2009.
- Mazoyer, M. and Roudart, L.: *A history of world agriculture: from the neolithic age to current crisis*, Monthly Review Press, London, 2006.
- McLauchlan, K.: The Nature and Longevity of Agricultural Impacts on Soil Carbon and Nutrients: A Review, *Ecosystems*, 9, 1364–1382, doi:10.1007/s10021-005-0135-1, 2006.
- Mitchell, T. D. and Jones, P. D.: An improved method of constructing a database of monthly climate observations and associated

- high-resolution grids, *Int. J. Climatol.*, 25, 693–712, doi:10.1002/joc.1181, 2005.
- Monnin, E., Indermuhle, A., Dallenbach, A., Fluckiger, J., Stauffer, B., Stocker, T. F., Raynaud, D., and Barnola, J.-M.: Atmospheric CO₂ Concentrations over the Last Glacial Termination, *Science*, 291, 112–114, doi:10.1126/science.291.5501.112, 2001.
- Murphey, R.: Deforestation in Modern China, in: *Global Deforestation and the Nineteenth Century World Economy*, edited by: Tucker, R. P. and Richards, J. F., Duke University Press, Durham, N.C., 1983.
- Murty, D., Kirschbaum, M., Mcmurtrie, R., and Mcgilvray, H.: Does conversion of forest to agricultural land change soil carbon and nitrogen? a review of the literature, *Glob. Change Biol.*, 8, 105–123, doi:10.0000/026999498377872, 2002.
- Myhre, G., Highwood, E. J., Shine, K., and Stordal, F.: New estimates of radiative forcing due to well mixed greenhouse gases, *Geophys. Res. Lett.*, 25, 2715–2718, 1998.
- Neve, R. J. and Bird, D. K.: Effects of syn-pandemic fire reduction and reforestation in the tropical Americas on atmospheric CO₂ during European conquest, *Palaeogeogr. Palaeoclimatol.*, 264, 25–38, 2008.
- New, M., Hulme, M., and Jones, P.: Representing Twentieth-Century Space-Time Climate Variability. Part I: Development of a 1961–90 Mean Monthly Terrestrial Climatology, *J. Climate*, 12, 829–856, 1999.
- Ogle, S. M., Breidt, F. J., and Paustian, K.: Agricultural management impacts on soil organic carbon storage under moist and dry climatic conditions of temperate and tropical regions, *Biogeochemistry*, 72, 87–121, doi:10.1007/s10533-004-0360-2, 2005.
- Olofsson, J. and Hickler, T.: Effects of human land-use on the global carbon cycle during the last 6000 years, *Vegetation History and Archaeobotany*, 17, 605–615, doi:10.1007/s00334-007-0126-6, 2008.
- Peltier, W. R.: Ice-age paleotopography, *Science*, 265, 195–201, 1994.
- Pongratz, J., Reick, C., Raddatz, T., and Claussen, M.: A reconstruction of global agricultural areas and land cover for the last millennium, *Global Biogeochem. Cy.*, 22, GB3018, doi:10.1029/2007GB003153, 2008.
- Pongratz, J., Raddatz, T., Reick, C. H., Esch, M., and Claussen, M.: Radiative forcing from anthropogenic land cover change since A.D. 800, *Geophys. Res. Lett.*, 36, L02709, doi:10.1029/2008GL036394, 2009a.
- Pongratz, J., Reick, C. H., Raddatz, T., and Claussen, M.: Effects of anthropogenic land cover change on the carbon cycle of the last millennium, *Global Biogeochem. Cy.*, 23, GB4001, doi:10.1029/2009GB003488, 2009b.
- Pongratz, J., Reick, C. H., Raddatz, T., and Claussen, M.: Biogeophysical versus biogeochemical climate response to historical anthropogenic land cover change, *Geophys. Res. Lett.*, 37, L08702, doi:10.1029/2010GL043010, 2010.
- Prentice, I. C., Farquhar, G. D., Fasham, M. J., Goulden, M. I., Heimann, M., Jaramillo, V. J., Kheshgi, H. S., LeQuéré, C., Scholes, R. J., and Wallace, D. W. R.: The carbon cycle and atmospheric CO₂, in: *Climate Change 2001: The Scientific Basis. Contribution of Working Group I to the Third Assessment Report of the Intergovernmental Panel on Climate Change*, edited by: Houghton, J. T., Ding, Y., Griggs, D., Noguer, M., van der Linden, P., Dai, X., Maskell, K., and Johnson, C. A., Cambridge University Press, Cambridge, United Kingdom and New York, NY, USA, 183–237, 2001.
- Quinton, J. N., Govers, G., Van Oost, K., and Bardgett, R. D.: The impact of agricultural soil erosion on biogeochemical cycling, *Nat. Geosci.*, 3, 311–314, doi:10.1038/ngeo838, 2010.
- Ramankutty, N. and Foley, J. A.: Estimating historical changes in global land cover: Croplands from 1700 to 1992, *Global Biogeochem. Cy.*, 13, 997–1027, 1999.
- Ramankutty, N., Foley, J. A., and Olejniczak, N. J.: People on the Land: Changes in Global Population and Croplands during the 20th Century, *Ambio*, 31, 251–257, 2002.
- Ridgwell, A. J., Watson, A. J., Maslin, M. A., and Kaplan, J. O.: Implications of coral reef buildup for the controls on atmospheric CO₂ since the last glacial maximum, *Paleoceanography*, 18, 1083–1093, doi:10.1029/2003PA000893, 2003.
- Ruddiman, W. F.: The anthropogenic greenhouse era began thousands of years ago, *Climatic Change*, 61, 261–293, 2003.
- Ruddiman, W. F.: The early anthropogenic hypothesis: Challenges and responses, *Rev. Geophys.*, 45, RG4001, doi:10.1029/2006RG000207, 2007.
- Ruddiman, W. F. and Ellis, E. C.: Effect of per-capita land use changes on Holocene forest clearance and CO₂ emissions, *Quaternary Sci. Rev.*, 28, 3011–3015, doi:10.1016/j.quascirev.2009.05.022, 2009.
- Sarmiento, J. L., Gloor, M., Gruber, N., Beaulieu, C., Jacobson, A. R., Mikaloff Fletcher, S. E., Pacala, S., and Rodgers, K.: Trends and regional distributions of land and ocean carbon sinks, *Biogeosciences*, 7, 2351–2367, doi:10.5194/bg-7-2351-2010, 2010.
- Schurgers, G., Mikolajewicz, U., Gröger, M., Maier-Reimer, E., Vizzaño, M., and Winguth, A.: Dynamics of the terrestrial biosphere, climate and atmospheric CO₂ concentration during interglacials: a comparison between Eemian and Holocene, *Clim. Past*, 2, 205–220, doi:10.5194/cp-2-205-2006, 2006.
- Shevliakova, E., Pacala, S. W., Malyshev, S., Hurtt, G. C., Milly, P. C. D., Caspersen, J. P., Sentman, L. T., Fisk, J. P., Wirth, C., and Crevoisier, C.: Carbon cycling under 300 years of land use change: Importance of the secondary vegetation sink, *Global Biogeochem. Cy.*, 23, GB2022, doi:10.1029/2007GB003176, 2009.
- Siegenthaler, U. and Oeschger, H.: Biospheric CO₂ emissions during the past 200 years reconstructed by deconvolution of ice core data, *Tellus B*, 39, 140–154, 1987.
- Sitch, S., Smith, B., Prentice, I. C., Arneeth, A., Bondeau, A., Cramer, W., Kaplan, J. O., Levis, S., Lucht, W., Sykes, M. T., Thonicke, K., and Venevsky, S.: Evaluation of ecosystem dynamics, plant geography and terrestrial carbon cycling in the LPJ dynamic global vegetation model, *Glob. Change Biol.*, 9, 161–185, 2003.
- Soepboer, W., Sugita, S., and Lotter, A. F.: Regional vegetation-cover changes on the Swiss Plateau during the past two millennia: A pollen-based reconstruction using the REVEALS model, *Quaternary Sci. Rev.*, 29, 472–483, doi:10.1016/j.quascirev.2009.09.027, available at: <http://www.sciencedirect.com/science/article/B6VBC-4XMTFNN-1/2/128208ffa88afd040af9dbbb77a2f6>, 2010.
- Stocker, B.: Transient simulations of land use change in the Holocene - Separating the human impact from natural drivers of the carbon cycle, Master's thesis, Klima- und Umwelphysik,

- University of Bern, Switzerland, available at: <http://www.climatestudies.unibe.ch/students/theses/msc/17.pdf>, 2009.
- Strassmann, K. M., Joos, F., and Fischer, G.: Simulating effects of land use changes on carbon fluxes: past contributions to atmospheric CO₂ increases and future commitments due to losses of terrestrial sink capacity, *Tellus B*, 60, 583–603, doi:10.1111/j.1600-0889.2008.00340.x, 2008.
- Tarnocai, C., Canadell, J. G., Schuur, E. A. G., Kuhry, P., Mazhitova, G., and Zimov, S.: Soil organic carbon pools in the northern circumpolar permafrost region, *Global Biogeochem. Cy.*, 23, GB2023, doi:10.1029/2008GB003327, 2009.
- Trudinger, C. M., Enting, I. G., Rayner, P. J., and Francey, R. J.: Kalman filter analysis of ice core data 2. Double deconvolution of CO₂ and $\delta^{13}\text{C}$ measurements, *J. Geophys. Res.*, 107, 4423–4447, doi:10.1029/2001JD001112, 2002.
- Tschumi, T., Joos, F., Gehlen, M., and Heinze, C.: Deep ocean ventilation, carbon isotopes, marine sedimentation and the deglacial CO₂ rise, *Clim. Past Discuss.*, 6, 1895–1958, doi:10.5194/cpd-6-1895-2010, 2010.
- Wania, R.: Modelling northern peatland land surface processes, vegetation dynamics and methane emissions, Ph.D. thesis, University of Bristol, 25 pp., 2007.
- Williams, M.: *Deforesting the Earth – From Prehistory to Global Crisis*, University of Chicago Press, Chicago and London, 2003.
- Wu, H., Guo, Z., and Peng, C.: Land use induced changes of organic carbon storage in soils of China, *Glob. Change Biol.*, 9, 305–315, doi:10.1046/j.1365-2486.2003.00590.x, 2003.
- HYDE 3.1: Current and historical population and land cover data base, <http://www.pbl.nl/en/themesites/hyde/landusedata/landcover/index.html>, access: 24 September 2008.
- Yu, Z., Loisel, J., Brosseau, D., Beilman, d., and Hunt, S.: Global peatland dynamics since the Last Glacial Maximum, *Geophys. Res. Lett.*, 37, 1–5, doi:10.1029/2010GL043584, 2010.